

Photo-induced ordering and anchoring properties of azo-dye films

Alexei D. Kiselev,^{*} Vladimir Chigrinov,[†] and Dan Ding Huang[‡]

*Hong Kong University of Science and Technology,
Clear Water Bay, Kowloon, Hong Kong*

(Dated: May 1, 2019)

Abstract

We study both theoretically and experimentally anchoring properties of photoaligning azo-dye films in contact with a nematic liquid crystal depending on photo-induced ordering of azo-dye molecules. In the mean field approximation, we found that the bare surface anchoring energy linearly depends on the azo-dye order parameter and the azimuthal anchoring strength decays to zero in the limit of vanishing photo-induced ordering. From the absorption dichroism spectra measured in the azo-dye films that are prepared from the azo-dye derivative with polymerizable terminal groups (SDA-2) we obtain dependence of the dichroic ratio on the irradiation dose. We also measure the polar and azimuthal anchoring strengths in nematic liquid crystal (NLC) cells aligned by the azo-dye films and derive the anchoring strengths as functions of the dichroic ratio which is proportional to the photo-induced order parameter. Though linear fitting of the experimental data for both anchoring strengths gives reasonably well results, it, in contradiction with the theory, predicts vanishing of the azimuthal anchoring strength at certain non-zero value of the azo-dye order parameter. By using a simple phenomenological model we show that this discrepancy can be attributed to the difference between the surface and bulk order parameters in the films. The measured polar anchoring energy is found to be an order of magnitude higher than the azimuthal strength. Our theory suggests that the quadrupole term of the spherical harmonics expansion for the azo-dye – NLC intermolecular potential might be of importance for the understanding of this difference.

^{*}Present address: Institute of Physics of NASU, prospekt Nauki 46, 03028 Kyiv, Ukraine; Email address: kisel@mail.cn.ua

[†]Email address: eechigr@ust.hk

[‡]Email address: eehdx@ust.hk

I. INTRODUCTION

When a nematic liquid crystal (NLC) is brought into contact with an anisotropic substrate, the energy of the NLC molecules in the interfacial layer and thus the surface tension [the excess free energy per unit area] will be orientationally dependent. The anisotropic part of the surface tension — the so-called *anchoring energy* — gives rise to the phenomenon known as *anchoring*, i.e., surface induced alignment of the nematic director along the vector of preferential orientation referred to as the *easy axis*.

Over the past few decades anchoring properties of NLCs have been the subject of intense studies for both technological and more fundamental reasons. There are a number of surface ordering and anchoring transitions that were observed experimentally and were studied using different theoretical approaches [see, *e.g.*, Refs. [1, 2, 3] for reviews].

Technologically, producing substrates with anisotropic anchoring properties is of vital importance in the fabrication of liquid crystal electrooptic devices. The traditional technique widely used to align liquid crystal display cells involves mechanical rubbing of aligning layers. This method, however, has the well known difficulties related to physical damage, impurities, dust contamination and generation of electrostatic charge [4].

An alternative *photoalignment* technique avoiding the drawbacks of the mechanical surface treatment was suggested in Refs. [5, 6, 7]. It uses linearly polarized ultraviolet (UV) light to induce anisotropy of the angular distribution of molecules in a photosensitive film [8].

The photoalignment has been extensively studied in a number of different polymer systems such as dye doped polymer layers [5, 9], cinnamate polymer derivatives [6, 7, 10, 11, 12] and side chain azopolymers [13, 14, 15, 16, 17, 18, 19]. Light induced ordering in the photosensitive materials, though not being understood very well, can occur by a variety of photochemically induced processes. These typically may involve such transformations as photoisomerization, crosslinking, photodimerization and photodecomposition (a recent review can be found in Ref. [20]).

In this paper we examine anchoring properties of the films containing photochemically stable azo dye structures that were recently studied as new photoaligning materials for NLC cells [21, 22]. Dependence of the surface anchoring strengths on the photoinduced anisotropy will be of our primary interest.

More specifically, we are aimed to study the effects of the photoinduced ordering in azo-dye films on the polar and azimuthal anchoring energies. The key point is that the photoalignment technique provides a means for controlling the photoinduced ordering that affects anchoring properties of photoaligning layers by changing ordering of azo-dye molecules at the surface and, thus, the surface anchoring strengths.

Recently, the anchoring properties of aligning photopolymer layers in relation to the photoinduced ordering were studied experimentally in Ref. [23]. The relationship between the rubbing strength and the azimuthal anchoring energy was discussed in Ref. [24]

The photopolymer-NLC interface was also described theoretically in Refs. [25, 26] using a modified version of the variational mean field approach which is also known as the Maier-Saupe theory. By contrast, the azo-dye films have not yet received a proper attention and we intend to fill in the gap.

The paper is organized as follows. In Sec. II we apply the mean field theoretical approach [27, 28, 29] to express the surface anchoring energy in terms of the tensorial order parameters which characterize angular distribution of the azo-dye and NLC molecules at the interfacial boundary surface. The general result is then used to derive the expressions

for the azimuthal and polar anchoring strengths that, in addition to the order parameters, depend on the harmonics of the intermolecular potentials.

Experimental details are given in Sec. III. The polymerizable azo-dye monomer SDA-2 was used to prepare the photoaligning layers. Absorption dichroism spectra were measured in the films irradiated with linearly polarized UV light at various irradiation doses. Anchoring energy measurements were performed in NLC cells where NLC is sandwiched between the glass plates coated with the azo-dye film.

In Sec. IV we present the experimental results and apply the theory of Sec. II to interpret the data. Discussion and concluding remarks are given in Sec. V. Details on some technical results are relegated to appendices A-B.

II. THEORY

In this section we begin with introducing general notations and apply the mean-field approach to express the Landau-de Gennes surface free energy in terms of both azo-dye and NLC order parameters. Expressions for the azimuthal and polar anchoring strengths, W_ϕ and W_θ , are then derived from the orientationally dependent part of the surface energy in Sec. II C. In the concluding part of this section we consider effects of spatial variations of the azo-dye order parameter using a simple model formulated in Sec. II D.

A. Order parameter and dichroic ratio

Assuming that the unit vector, $\hat{\mathbf{u}} = (\sin\theta\cos\phi, \sin\theta\sin\phi, \cos\theta)$, directed along the long molecular axis defines orientation of a molecule in both azo-dye film and NLC cell, quadrupolar orientational ordering of the molecules can be characterized using the traceless symmetric second-rank tensor [30]

$$\mathbf{Q}(\hat{\mathbf{u}}) = (3\hat{\mathbf{u}} \otimes \hat{\mathbf{u}} - \mathbf{I})/2, \quad (1)$$

where \mathbf{I} is the identity matrix. The dyadic (1) averaged over orientation of molecules with the one-particle distribution function $\rho_\alpha(\mathbf{r}, \hat{\mathbf{u}})$, describing the orientation-density profile of azo-dye ($\alpha = A$) and NLC ($\alpha = N$) molecules, is proportional to the *order parameter tensor* $\mathbf{S}_\alpha(\mathbf{r})$

$$\int \rho_\alpha(\mathbf{r}, \hat{\mathbf{u}}) \mathbf{Q}(\hat{\mathbf{u}}) d\hat{\mathbf{u}} = \rho_\alpha(\mathbf{r}) \mathbf{S}_\alpha(\mathbf{r}), \quad (2)$$

where $d\hat{\mathbf{u}} \equiv \sin\theta d\theta d\phi$, $\rho_\alpha(\mathbf{r}, \hat{\mathbf{u}}) = \rho_\alpha(\mathbf{r}) f_\alpha(\mathbf{r}, \hat{\mathbf{u}})$, $\rho_\alpha(\mathbf{r}) = \int \rho_\alpha(\mathbf{r}, \hat{\mathbf{u}}) d\hat{\mathbf{u}}$ is the density profile and $f_\alpha(\mathbf{r}, \hat{\mathbf{u}})$ is the normalized angular distribution. The general expression for the order parameter is given in appendix A [see Eq. (A15)] along with technical details on the technique of irreducible tensors.

Now we dwell briefly on the relation between the order parameter \mathbf{S}_A characterizing orientational distribution of azo-dye molecules $f_A(\hat{\mathbf{u}})$ and the absorption dichroic ratio

$$R = \frac{D_\parallel - D_\perp}{D_\parallel + 2D_\perp}, \quad (3)$$

where D_\parallel [D_\perp] is the absorption coefficient measured for a testing beam linearly polarized parallel [perpendicular] to the polarization vector of the activating UV light which is directed

along the x axis, $\mathbf{E}_{\text{ex}} = E_{\text{ex}} \hat{\mathbf{x}}$. We shall also assume that the testing and the pumping waves are both propagating along the z axis which is normal to the film substrate.

When the absorption tensor of an azo-dye molecule is uniaxially anisotropic with $\sigma_{ij}(\hat{\mathbf{u}}) = \sigma_{\perp} \delta_{ij} + (\sigma_{\parallel} - \sigma_{\perp}) u_i u_j$, its orientational average takes the following matrix form

$$\langle \boldsymbol{\sigma} \rangle = (\sigma_{\text{av}} \mathbf{I} + 2 \Delta\sigma \mathbf{S}_A)/3, \quad (4)$$

$$\sigma_{\text{av}} = \sigma_{\parallel} + 2\sigma_{\perp}, \quad \Delta\sigma = \sigma_{\parallel} - \sigma_{\perp}, \quad (5)$$

where the angular brackets $\langle \dots \rangle$ denote orientational averaging.

In the low concentration approximation, the optical densities D_{\parallel} and D_{\perp} are proportional to the corresponding components of the tensor (4)

$$D_{\parallel} \propto \rho_A (\sigma_{\text{av}} + 2 \Delta\sigma S_{xx}^{(A)})/3, \quad (6)$$

$$D_{\perp} \propto \rho_A (\sigma_{\text{av}} + 2 \Delta\sigma S_{yy}^{(A)})/3, \quad (7)$$

so that the average absorption coefficient D_{av} is given by

$$D_{\text{av}} = D_{\parallel} + 2D_{\perp} \propto \rho_A (\sigma_{\text{av}} + 2/3 \Delta\sigma [S_{yy}^{(A)} - S_{zz}^{(A)}]). \quad (8)$$

When the absorption coefficient D_{av} does not depend on irradiation dose (and, thus, on the order parameter), from the expression (8) we may conclude that anisotropy of the azo-dye film is uniaxial and $S_{yy}^{(A)} = S_{zz}^{(A)} = -S_{xx}^{(A)}/2 \equiv -S_A/2$. In this case we have

$$\mathbf{S}_A = S_A(3 \hat{\mathbf{x}} \otimes \hat{\mathbf{x}} - \mathbf{I})/2, \quad R = \frac{\Delta\sigma}{\sigma_{\text{av}}} S_A. \quad (9)$$

As is seen from Eq. (9), the dichroic ratio equals the order parameter only in the limiting case where absorption of waves propagating along the long molecular axis is negligibly small and $\sigma_{\perp} \rightarrow 0$.

B. Anisotropic part of surface energy in the mean-field approximation

In the previous section it was shown that the light induced ordering of azo-dye molecules can be described by the order parameter (9) which is expected to affect the surface free energy at the nematic-substrate interface. So, in this section, the order parameter dependent part of the surface energy will be of our primary concern.

In the case of a flat structureless substrate, the expression for the surface energy was originally obtained by Sen and Sullivan in Ref. [27]. Subsequently, similar results have been derived by using the mean-field approximation [28] and the density functional theory [31, 32, 33].

Similarly to Ref. [28], we adopt the mean-field approach and use the Fowler approximation for the one-particle distribution functions

$$\rho_N(\mathbf{r}, \hat{\mathbf{u}}) = H(z)\rho_N(z, \hat{\mathbf{u}}), \quad \rho_A(\mathbf{r}, \hat{\mathbf{u}}) = H(-z)\rho_A(z, \hat{\mathbf{u}}), \quad (10)$$

where $H(z)$ is the Heaviside step function which equals unity when z is positive and vanishes otherwise.

Applying the mean-field theory [28] gives the Landau-de Gennes surface free energy as an excess Helmholtz free energy per unit area that depends on two pair intermolecular

potentials: (a) the potential of interaction between NLC molecules, $U_{N-N}(\mathbf{r}_{12}, \hat{\mathbf{u}}_1, \hat{\mathbf{u}}_2)$; and (b) the potential of interaction between NLC and azo-dye molecules, $U_{A-N}(\mathbf{r}_{12}, \hat{\mathbf{u}}_1, \hat{\mathbf{u}}_2)$, where $\mathbf{r}_{12} = \mathbf{r}_1 - \mathbf{r}_2$ is the vector of intermolecular separation and $\hat{\mathbf{u}}_i$ is the orientation coordinates of the interacting molecules. The resulting expression is given by

$$\begin{aligned} \Delta F/A &= \int_{-\infty}^0 dz_1 \int_0^{\infty} dz_2 \int d\hat{\mathbf{u}}_1 d\hat{\mathbf{u}}_2 \\ &\times \left[\rho_A(z_1, \hat{\mathbf{u}}_1) V_A(z_{12}, \hat{\mathbf{u}}_1, \hat{\mathbf{u}}_2) \rho_N(z_2, \hat{\mathbf{u}}_2) \right. \\ &\left. - \frac{1}{2} \rho_N(z_1, \hat{\mathbf{u}}_1) V_N(z_{12}, \hat{\mathbf{u}}_1, \hat{\mathbf{u}}_2) \rho_N(z_2, \hat{\mathbf{u}}_2) \right], \end{aligned} \quad (11)$$

$$V_\alpha(z_{12}, \hat{\mathbf{u}}_1, \hat{\mathbf{u}}_2) = \int_A U_{\alpha-N}(\mathbf{r}_{12}, \hat{\mathbf{u}}_1, \hat{\mathbf{u}}_2) dx_{12} dy_{12}, \quad (12)$$

where A is the area of the substrate and V_α is the potential averaged over in-plane coordinates.

It should be noted that the potentials U_{N-N} and U_{A-N} actually represent the perturbative part of interaction that can be treated in the mean-field approximation. They can be written in the form of expansion over spherical harmonics given in Eq. (B1) of appendix B. For our purposes, however, it is more convenient to use the tensorial representation for the averaged potentials V_α that was introduced in Ref. [34]. In appendix B, the coefficients that enter this representation [see Eq. (B4)] are related to the coefficients, $v_{j_1 j_2 j}(z)$ with $j_i < 4$, in the spherical harmonics expansion (B4). This relation is given by Eqs. (B9)–(B12).

Substituting the representation (B4) into Eq. (11) and assuming homogeneity of the contacting phases, we obtain the Landau-de Gennes expression for the surface free energy in the final form:

$$f_S(\mathbf{S}_N, \mathbf{S}_A) = f_N(\mathbf{S}_N) + f_A(\mathbf{S}_N, \mathbf{S}_A), \quad (13)$$

$$\begin{aligned} f_N(\mathbf{S}_N) &= c_0 \hat{\mathbf{z}} \cdot \mathbf{S}_N \cdot \hat{\mathbf{z}} + c_N^{(1)} \text{Tr}(\mathbf{S}_N^2) \\ &+ c_N^{(2)} \hat{\mathbf{z}} \cdot \mathbf{S}_N^2 \cdot \hat{\mathbf{z}} + c_N^{(3)} [\hat{\mathbf{z}} \cdot \mathbf{S}_N \cdot \hat{\mathbf{z}}]^2, \end{aligned} \quad (14)$$

$$\begin{aligned} f_A(\mathbf{S}_N, \mathbf{S}_A) &= c_A^{(1)} \text{Tr}(\mathbf{S}_N \mathbf{S}_A) \\ &+ c_A^{(2)} \hat{\mathbf{z}} \cdot \mathbf{S}_N \mathbf{S}_A \cdot \hat{\mathbf{z}} + c_A^{(3)} [\hat{\mathbf{z}} \cdot \mathbf{S}_N \cdot \hat{\mathbf{z}}] \cdot [\hat{\mathbf{z}} \cdot \mathbf{S}_A \cdot \hat{\mathbf{z}}], \end{aligned} \quad (15)$$

where the coefficients are given by

$$c_0 = b_A^{(0)} - b_N^{(0)}, \quad (16)$$

$$c_A^{(i)} = b_A^{(i)}, \quad c_N^{(i)} = -b_N^{(i)}/2, \quad (17)$$

$$b_\alpha^{(i)} = \rho_\alpha \rho_N \int_0^\infty z \beta_\alpha^{(i)}(z) dz, \quad (18)$$

$\beta_\alpha^{(i)}(z)$ denote the coefficients in the representation (B4) for the potential (12).

Eqs. (13)–(15) can be viewed as a generalization of the expression by Sen and Sullivan [27] supplemented with the term $f_A(\mathbf{S}_N, \mathbf{S}_A)$ resulting from the interaction between NLC and azo-dye molecules. Note that this result can also be derived by constructing invariants from the order parameter tensors \mathbf{S}_α and the normal to the substrate $\hat{\mathbf{z}}$. In this case, the surface of the azo-dye aligning film is treated phenomenologically as a bounding surface which, in addition to the normal $\hat{\mathbf{z}}$, is characterized by the order parameter \mathbf{S}_A .

C. Bare anchoring energy

Separating out the director dependent part of the surface free energy requires the order parameters of azo-dye and NLC molecules be substituted into Eqs. (13)–(15). Since the order parameter at the surface may differ from its value in the bulk, we generalize the expression for the azo-dye order parameter (9) as follows

$$2\mathbf{S}_A|_{z=0} = S_A(3\hat{\mathbf{x}} \otimes \hat{\mathbf{x}} - \mathbf{I}) + P_A(\hat{\mathbf{z}} \otimes \hat{\mathbf{z}} - \hat{\mathbf{y}} \otimes \hat{\mathbf{y}}). \quad (19)$$

Similarly, for NLC order parameter tensor at $z = 0$, from Eq. (A15) we have

$$\begin{aligned} 2\mathbf{S}_N|_{z=0} &= S(3\hat{\mathbf{n}} \otimes \hat{\mathbf{n}} - \mathbf{I}) + P(\hat{\mathbf{m}} \otimes \hat{\mathbf{m}} - \hat{\mathbf{l}} \otimes \hat{\mathbf{l}}) \\ &= (3S + P)\hat{\mathbf{n}} \otimes \hat{\mathbf{n}} + 2P\hat{\mathbf{m}} \otimes \hat{\mathbf{m}} - (S + P)\mathbf{I}, \end{aligned} \quad (20)$$

where $\hat{\mathbf{n}} = (\sin \Theta \cos \Phi, \sin \Theta \sin \Phi, \cos \Theta)$ is the NLC director, $\hat{\mathbf{n}} \perp \hat{\mathbf{m}} = \cos \gamma \mathbf{e}_x(\hat{\mathbf{n}}) - \sin \gamma \mathbf{e}_y(\hat{\mathbf{n}})$, $\mathbf{e}_x(\hat{\mathbf{n}}) = (\cos \Theta \cos \Phi, \cos \Theta \sin \Phi, -\sin \Theta)$, $\mathbf{e}_y(\hat{\mathbf{n}}) = (-\sin \Phi, \cos \Phi, 0)$ and $\hat{\mathbf{l}} = \hat{\mathbf{n}} \times \hat{\mathbf{m}}$.

Eqs. (19) and (20) suggest that the order parameters of azo-dye and NLC molecules though being both uniaxial in the bulk can be biaxial at the surface. In addition, the scalar order parameters S_A and S at the surface may also deviate from their values in the bulk.

The surface free energy can now be expressed as a sum of two contributions

$$f_S(\mathbf{S}, \mathbf{S}_A) = W(\hat{\mathbf{n}}, \hat{\mathbf{m}}) + f_{\text{scal}}, \quad (21)$$

where $W(\hat{\mathbf{n}}, \hat{\mathbf{m}})$ is the orientationally dependent part of the surface energy. This part can be calculated by substituting the order parameters (19) and (20) into the surface energy (13) to yield the expression for the bare anchoring energy

$$\begin{aligned} W(\hat{\mathbf{n}}, \hat{\mathbf{m}}) &= N_z(\hat{\mathbf{n}} \cdot \hat{\mathbf{z}})^2 + M_z(\hat{\mathbf{m}} \cdot \hat{\mathbf{z}})^2 \\ &+ N_x(\hat{\mathbf{n}} \cdot \hat{\mathbf{x}})^2 + M_x(\hat{\mathbf{m}} \cdot \hat{\mathbf{x}})^2 \\ &+ c_N^{(3)}/4 \left[(3S + P)(\hat{\mathbf{n}} \cdot \hat{\mathbf{z}})^2 + 2P(\hat{\mathbf{m}} \cdot \hat{\mathbf{z}})^2 \right]^2 \end{aligned} \quad (22)$$

with the coefficients defined by the relations:

$$4N_z = (3S + P)[q + c_N^{(2)}(S - P)], \quad (23)$$

$$4N_x = c_A^{(1)}(3S_A + P_A)(3S + P), \quad (24)$$

$$2M_z = P[q - 2c_N^{(2)}S], \quad 2M_x = c_A^{(1)}(3S_A + P_A)P, \quad (25)$$

$$q \equiv 2c_0 - (c_A^{(2)} + c_A^{(3)})(S_A - P_A) + 2c_A^{(1)}P_A - 2c_N^{(3)}(S + P). \quad (26)$$

The second term on the right hand side of Eq. (21)

$$\begin{aligned} 4f_{\text{scal}} &= -[2c_0 - (S_A - P_A)(c_A^{(2)} + c_A^{(3)}) + 3c_A^{(1)}(S_A + P_A)] \\ &\times (S + P) + (c_N^{(2)} + c_N^{(3)})(S + P)^2 + 2c_N^{(1)}(3S^2 + P^2). \end{aligned} \quad (27)$$

is a quadratic function of NLC scalar order parameter S and the biaxiality P . From Eq. (27) it, similarly to the anchoring energy (22), depends linearly on the azo-dye parameters S_A and P_A .

For the anchoring energy (22), we consider the simplest case which occurs when the surface induced NLC biaxiality P is negligibly small and the quadrupolar term v_{224} in the expansion of the intermolecular potential V_N can be ignored. Under these circumstances, setting $P = c_N^{(3)} = 0$ and $M_z = M_x = 0$, we arrive at the simplified formula for the anchoring energy

$$W(\hat{\mathbf{n}}) = N_z(\hat{\mathbf{n}} \cdot \hat{\mathbf{z}})^2 + N_x(\hat{\mathbf{n}} \cdot \hat{\mathbf{x}})^2 \quad (28)$$

which agrees with the expression for the anchoring energy recently proposed in Refs. [35, 36, 37].

From Eq. (28) it is clear that the easy axis is directed along the y axis, $\mathbf{e}_s = \hat{\mathbf{y}}$, only if the coefficients N_z and N_x are both positive. In this case the polar and the azimuthal anchoring strengths, W_θ and W_ϕ , are given by

$$W_\theta = 2N_z, \quad W_\phi = 2N_x. \quad (29)$$

From Eq. (24) we immediately deduce a more explicit expression for the azimuthal anchoring strength

$$W_\phi = w_\phi [S_{yy}^{(A)}|_{z=0} - S_{xx}^{(A)}|_{z=0}], \quad (30)$$

$$2w_\phi = -3c_A^{(1)} S|_{z=0}, \quad (31)$$

where notations indicate the plane $z = 0$ as a surface separating the phases.

Similarly, Eq. (23) gives the polar anchoring strength in the explicit form

$$W_\theta = w_\theta^{(0)} + w_\theta^{(1)} S_{zz}^{(A)}|_{z=0} - w_\phi [S_{zz}^{(A)}|_{z=0} - S_{yy}^{(A)}|_{z=0}], \quad (32)$$

$$2w_\theta^{(1)} = 3(c_A^{(2)} + c_A^{(3)}) S|_{z=0}. \quad (33)$$

The formulas (30)-(33) will be subsequently used in Sec. IV to interpret the experimental data. At this stage, it is worth noting that, for the order parameter (9), the relations (31) and (33) provide the inequalities

$$c_A^{(1)} < 0, \quad c_A^{(2)} + c_A^{(3)} > 0 \quad (34)$$

as conditions for the anchoring strengths to increase linearly as the scalar order parameter S_A decreases.

D. Model of spatially varying order parameter

As it was pointed out at the beginning of the previous section, the surface order parameter tensor of an azo-dye film (19) may differ from the bulk order parameter of the film (9). The latter, according to the experimental results presented in the subsequent section III, is uniaxially anisotropic with the in-plane anisotropy axis that is normal to the polarization vector of the activating UV light. In addition, the light induced scalar order parameter, which is proportional to the dichroic ratio (3), turns out to be negative, $S_A^{(b)} < 0$.

From the other hand, assuming that the anisotropic part of the surface energy can be taken in the general form by Sen and Sullivan [27], the boundary conditions may favor either homeotropic or planar alignment of the azo-dye molecules, thus, counteracting the action of

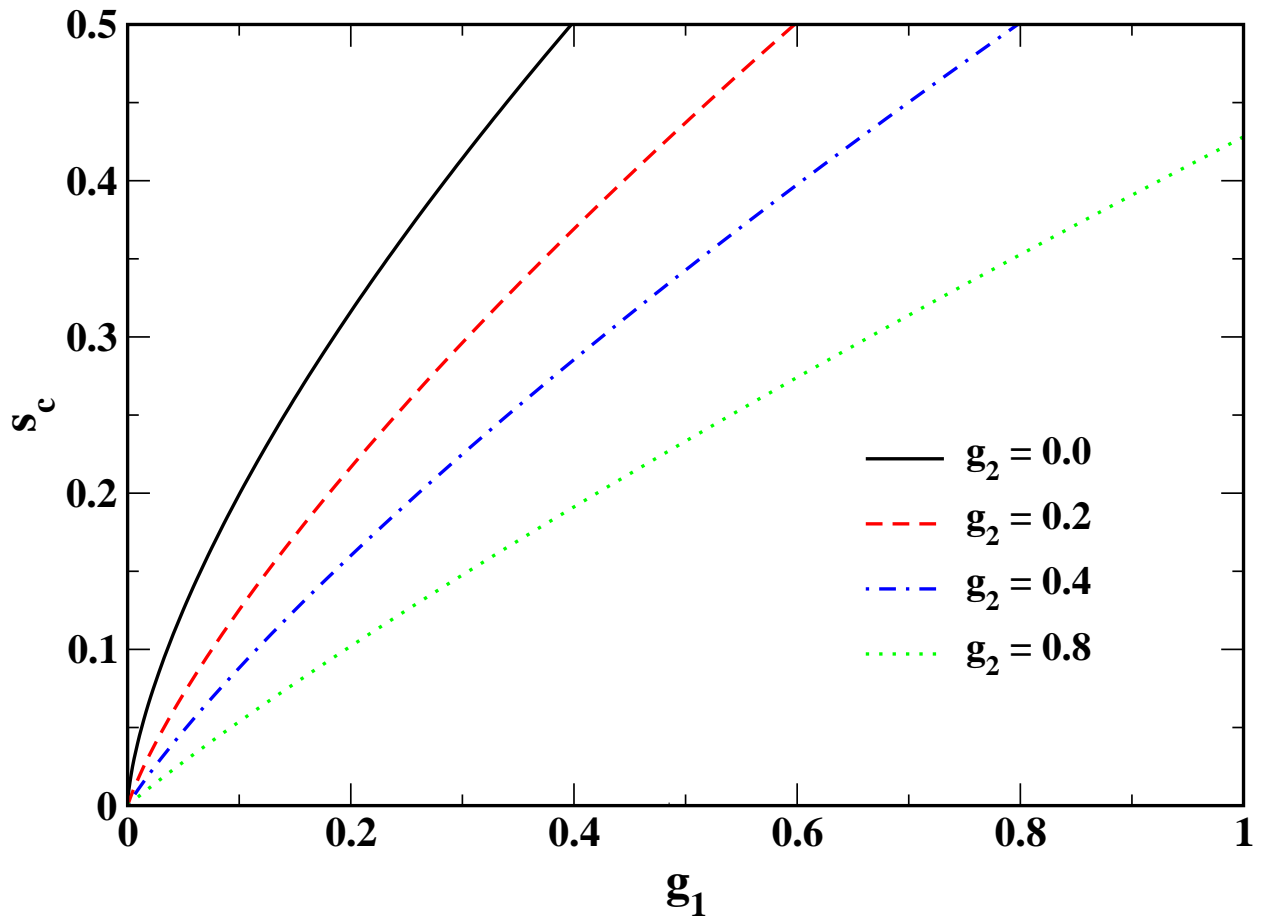


FIG. 1: Critical order parameter s_c as a function of the coupling constant g_1 at various values of the coefficient g_2 .

light. So, it can be expected that the effects caused by interplay between the light induced and the surface ordering are of importance in explaining the order parameter dependencies of the polar and azimuthal anchoring energies.

In this section we discuss these effects on the basis of a simple phenomenological model formulated by using the polar representation (A21) for the azo-dye order parameter. The latter can be conveniently rewritten in the form

$$S_A = -s_A \cos \psi, \quad P_A = -\sqrt{3} s_A \sin \psi, \quad (35)$$

where the angle ψ is shifted by π so as to have the angle ψ vanishing in the bulk.

In what follows we shall assume that, similarly to nematic liquid crystals [38, 39, 40, 41], the amplitude s_A varies in space much slower than the angle ψ . So, in our model, the amplitude will be fixed at its bulk value, $s_A = |S_A^{(b)}|$, and we consider the limiting case of thick films in which the characteristic length of spatial variations of the angle ψ is much shorter than the film thickness. In this case the film can be regarded as a semi-infinite sample filling the upper half space, $z \geq 0$.

Technically, our task will be to find the spatially varying angle ψ as a function of z that

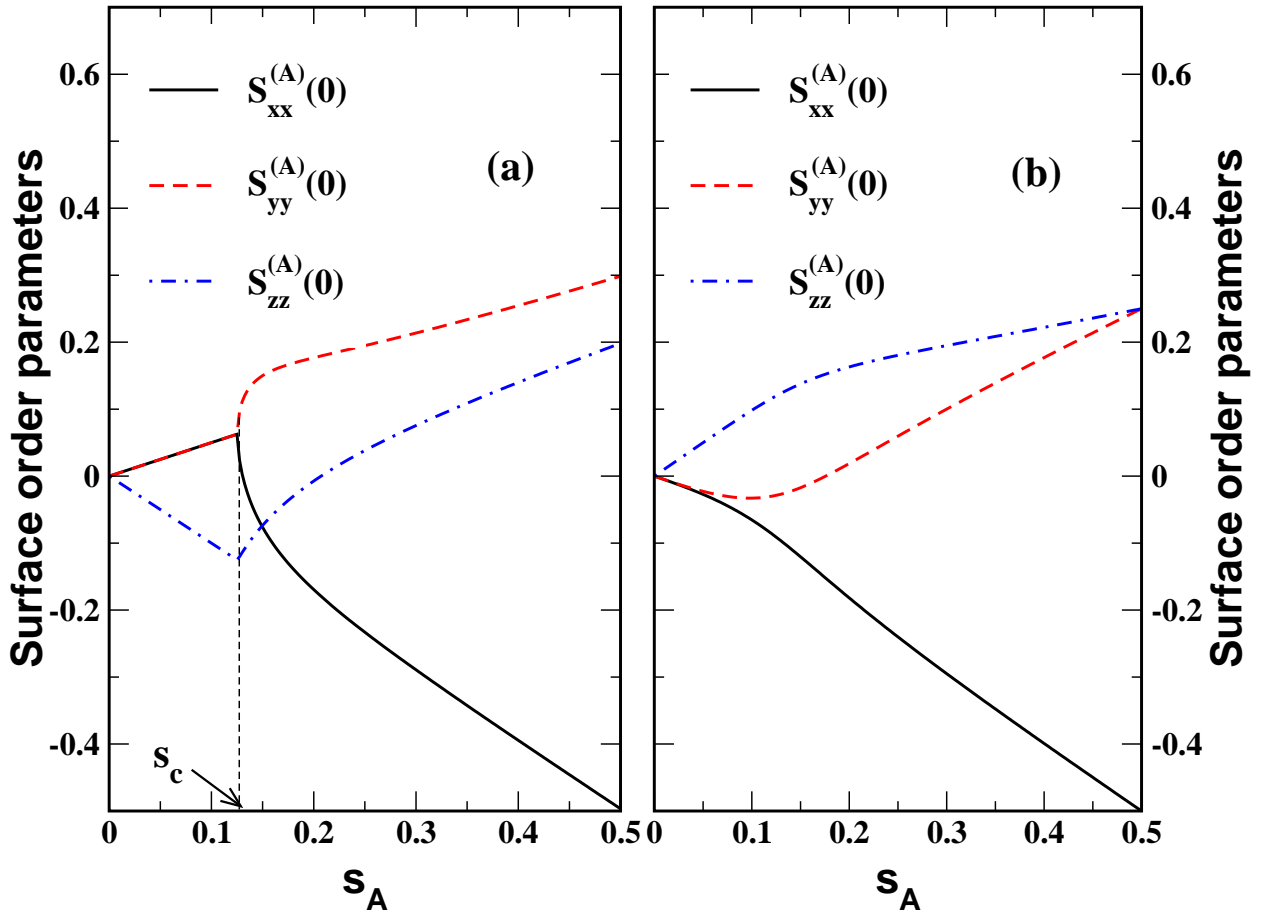


FIG. 2: Components of the order parameter at the surface as functions of the bulk order parameter s_A . Two cases are shown: (a) $g_1 = 0.05$ and $g_2 = 0.0$; (b) $g_1 = -0.2$ and $g_2 = 0.4$.

minimizes the excess free energy per unit area, F_A , taken in the following nematic-like form

$$F_A = \int_0^\infty \left[L s_A^2 (\partial_z \psi)^2 + B s_A^3 (1 - \cos(3\psi)) \right] dz + G_1 s_A \cos(\psi_0 + \pi/3) + G_2 s_A^2 \cos^2(\psi_0 + \pi/3), \quad (36)$$

where $\psi_0 \equiv \psi|_{z=0}$ and $s_A \cos(\psi_0 + \pi/3) = \hat{\mathbf{z}} \cdot \mathbf{S}_A \cdot \hat{\mathbf{z}}|_{z=0}$. The first part of the excess free energy (36) is of integral form with the integrand describing the energy costs for deviations of ψ from the equilibrium value, $\psi = 0$. The gradient term of the energy density is taken to be proportional to $(\partial_z \mathbf{S}_A)^2$, whereas the other term gives an increase in energy caused by spatially uniform changes in ψ . This term is written as a linear function of the angle dependent invariant (A19), $4 \text{Tr}[\mathbf{S}_A^3] = 3s_A^3 \cos(3\psi)$.

For the order parameter (19), the surface part of the energy (36) can be represented by a quadratic polynomial of $\hat{\mathbf{z}} \cdot \mathbf{S}_A \cdot \hat{\mathbf{z}}$. By contrast to the elastic constant L and the coefficient B , the surface coupling constants, G_1 and G_2 , can generally be negative leading to different boundary conditions. For example, if $G_2 = 0$, minimizing the surface term requires the z -component of the order parameter, $\hat{\mathbf{z}} \cdot \mathbf{S}_A \cdot \hat{\mathbf{z}} = S_{zz}^{(A)}$, to attain its maximal (minimal) value at the surface provided the coefficient G_1 is negative (positive). These can be referred to as the homeotropic (planar) boundary conditions.

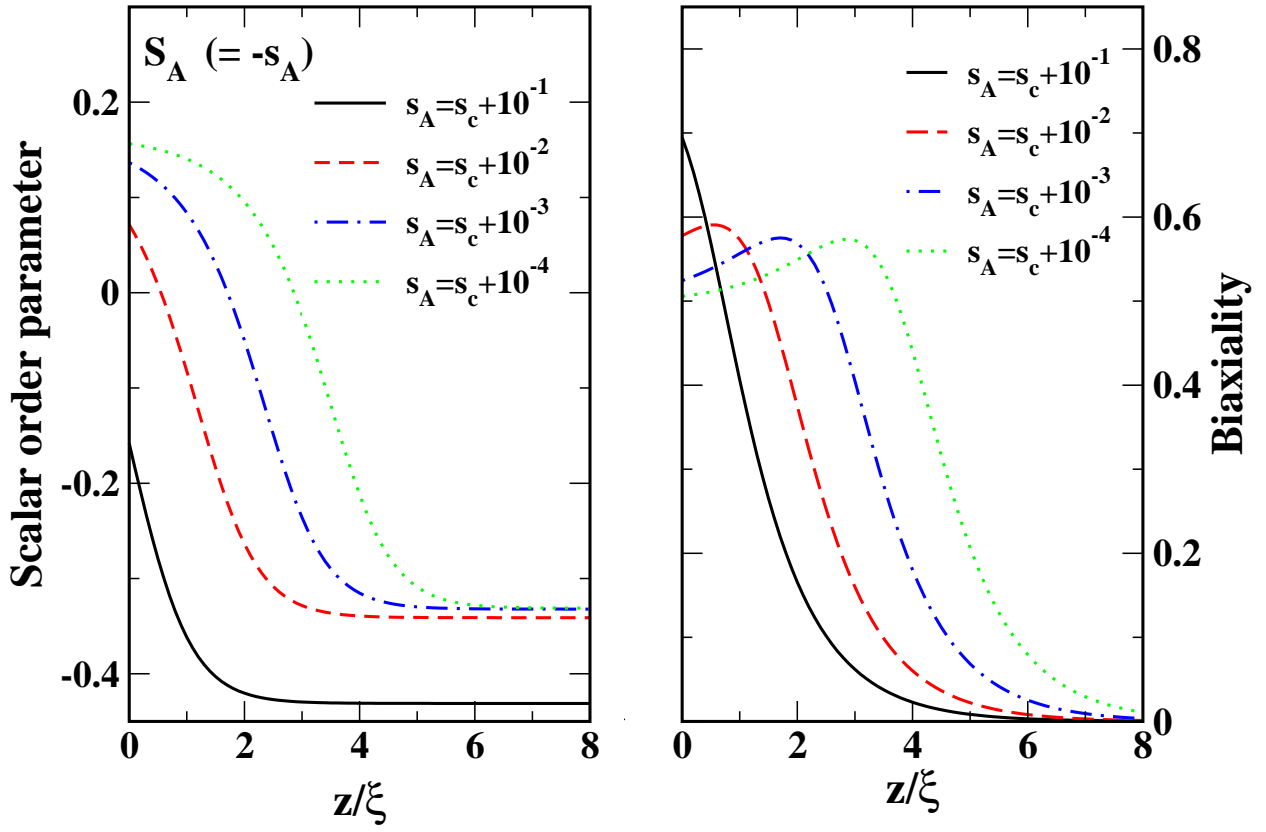


FIG. 3: (a) Scalar order parameter and (b) biaxiality in relation to the ratio z/ξ .

The Euler-Lagrange equation for the free energy functional (36) can be readily solved to yield the relation

$$\tan(3\psi/4) = \tan(3\psi_0/4) \exp(-z/\xi), \quad (37)$$

where $9\xi^2 = 2L(Bs_A)^{-1}$. This relation can now be substituted into Eq. (36) to derive the free energy as a function of the angle ψ_0 . The result is

$$F_A/h \equiv \tilde{f}_A(\psi_0) = s_A^{5/2} \sin^2(3\psi_0/4) + g_1 s_A \cos(\psi_0 + \pi/3) + g_2 s_A^2 \cos^2(\psi_0 + \pi/3), \quad (38)$$

where $h = 4(2BL)^{1/2}/3$ and $g_i = G_i/h$. The angle ψ at the surface then can be found as the value of ψ_0 that minimizes the function (38) on the interval ranged from $-\pi/3$ to $2\pi/3$.

Qualitatively, dependence of ψ_0 on the coupling constant g_1 can be analyzed using elementary methods. For $g_2 \geq 0$, we find that the angle ψ_0 is localized within different intervals depending on the value of g_1 . These are given by

$$\begin{cases} -\pi/3 < \psi_0 \leq 0, & g_1 \leq g_c^{(1)} = -g_2 s_A, \\ 0 < \psi_0 \leq \pi/3, & g_c^{(1)} < g_1 \leq g_c^{(2)} = g_2 s_A + \sqrt{3}/2 s_A^{3/2}, \\ \pi/3 < \psi_0 \leq 2\pi/3, & g_c^{(2)} < g_1 \leq g_c^{(3)} = 2g_2 s_A + 9/8 s_A^{3/2}, \\ \psi_0 = 2\pi/3, & g_1 > g_c^{(3)}. \end{cases} \quad (39)$$

The end points of the intervals in Eq. (39), $\psi_0 = k\pi/3$ with $-1 \leq k \leq 2$, represent the uniaxially anisotropic structures at the surface

$$\mathbf{S}_A(0) = s_A(3\hat{z} \otimes \hat{z} - \mathbf{I})/2, \quad \psi_0 = -\pi/3, \quad (40)$$

$$\mathbf{S}_A(0) = -s_A(3\hat{x} \otimes \hat{x} - \mathbf{I})/2, \quad \psi_0 = 0, \quad (41)$$

$$\mathbf{S}_A(0) = s_A(3\hat{y} \otimes \hat{y} - \mathbf{I})/2, \quad \psi_0 = \pi/3, \quad (42)$$

$$\mathbf{S}_A(0) = -s_A(3\hat{z} \otimes \hat{z} - \mathbf{I})/2, \quad \psi_0 = 2\pi/3. \quad (43)$$

From Eqs. (40) and (42) it is seen that, for the angles $\psi_0 = -\pi/3$ and $\psi_0 = \pi/3$, surface alignment will be homeotropic and homogeneous (monostable planar), respectively. The structure (41) coincides with uniaxial ordering in the bulk (9) and the surface order parameter tensor (43) corresponds to planar (random in-plane) alignment.

According to Eq. (39), the case of planar alignment occurs only if the coupling constant g_1 is positive and the bulk order parameter s_A is below its critical value s_c defined by the relation

$$g_1 = 2g_2s_c + 9/8 s_c^{3/2}. \quad (44)$$

Fig. 1 shows that the critical order parameter s_c is an increasing function of g_1 .

In Fig. 2(a) we have plotted the curves representing the components of the order parameter tensor at the surface in relation to the order parameter in the bulk to illustrate that destruction of the planar alignment takes place in a second order transition manner.

However, it should be stressed that our model becomes inapplicable in the immediate vicinity of s_c where z -dependence of the biaxiality parameter P_A critically slows down. Actually, as it can be inferred from Fig. 3, the characteristic length of spatially varying biaxiality diverges logarithmically as s_A approaches s_c from above. Under these circumstances, the assumption that scale of the spatial variations is much shorter than the film thickness is no more justified.

By contrast to the boundary conditions with $g_1 > 0$, there are no second order transitions provided the coupling constant g_1 is negative. At sufficiently large values of $|g_1|$, the surface ordering remains nearly homeotropic. Otherwise, the surface order parameter changes smoothly with s_A towards the bulk order parameter (41). From Eq. (39), for $g_1 = -g_2s_A$, difference between the order parameters vanishes. The curves presented in Fig. 2(b) illustrate this point.

Leaving aside a detailed discussion of what happens when the coupling constant g_2 is negative, we just note that in this case the above discussed transition will generally be first order leading to jump-like behavior of the order parameter at the surface.

III. EXPERIMENT

Now we pass on to describing the experimental procedure employed to obtain the data linking the anchoring energy strengths and the dichroic ratio as a measure of the photo-induced ordering. To this end we carried out the absorption spectra and the anchoring energy measurements for the azo-dye films irradiated at varying exposure time. Thus, we used the samples prepared at different irradiation doses to measure the anchoring strengths and the dichroic ratio in relation to the dose. The data then can be recalculated to obtain the required anchoring energy vs dichroic ratio dependence.

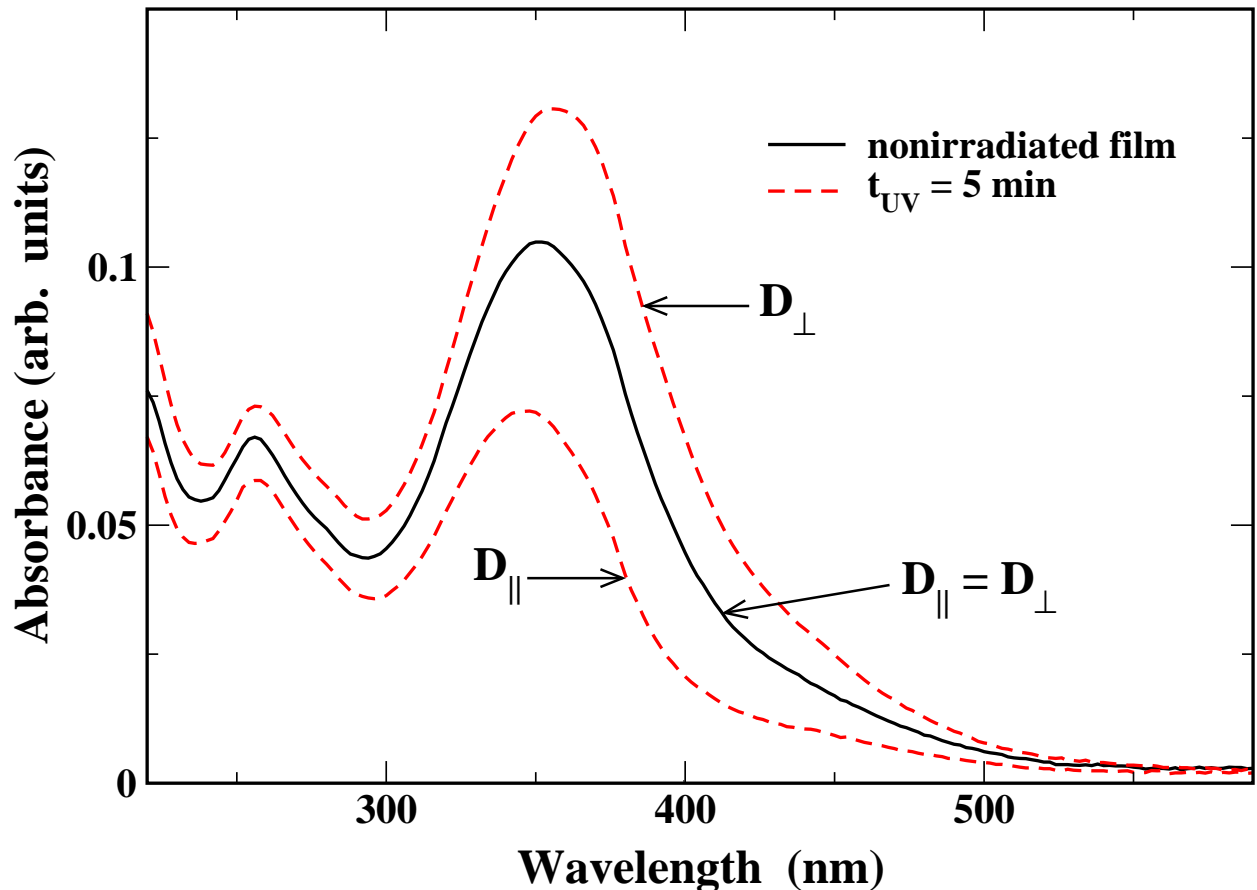


FIG. 4: UV-visible absorption spectra of nonirradiated and irradiated azo-dye films.

A. Sample preparation

Following the method described in Ref. [21], the azobenzene sulfuric dye SD-1 was synthesized from corresponding benzidinedisulfonic acid using azo coupling. The azo-dye compound SD-1 was mixed with the polymerizable azo-dye SDA-2 in the ratio 40% to 60%. The mixture was dissolved in N,N-dimethylformamide (DMF) and a heat initiator V-65 (from Wako pure chemical industries, Ltd.) that was added in relation of 1:50 to SDA-2.

The solution was spin-coated onto glass substrates with indium-tin-oxide (ITO) electrodes at 800 rpm for 5 seconds and, subsequently, at 3000 rpm for 30 seconds. The solvent was evaporated on a hot plate at 100°C for 10 minutes.

The surface of the coated film was illuminated with linearly polarized UV light using super-high pressure Hg lamp through an interference filter at the wavelength 365 nm. The intensity of light irradiated on the film surface at varying time exposure was 2.7 mW/cm². After the photoalignment procedure, the SDA-2 films were polymerized by heating at 150°C for 1 hour in vacuum. In order to recover quality of the photoalignment degraded after the polymerization, the films were exposed to the UV light for 1 minute regardless of the initial time exposure.

Two glass substrates with the photoaligned films were assembled to form liquid crystal cells to measure the azimuthal and polar anchoring energy strengths. The cell thickness was 5 μm and 18 μm , respectively. Liquid crystal mixtures MLC-6080 (from Merck) in an

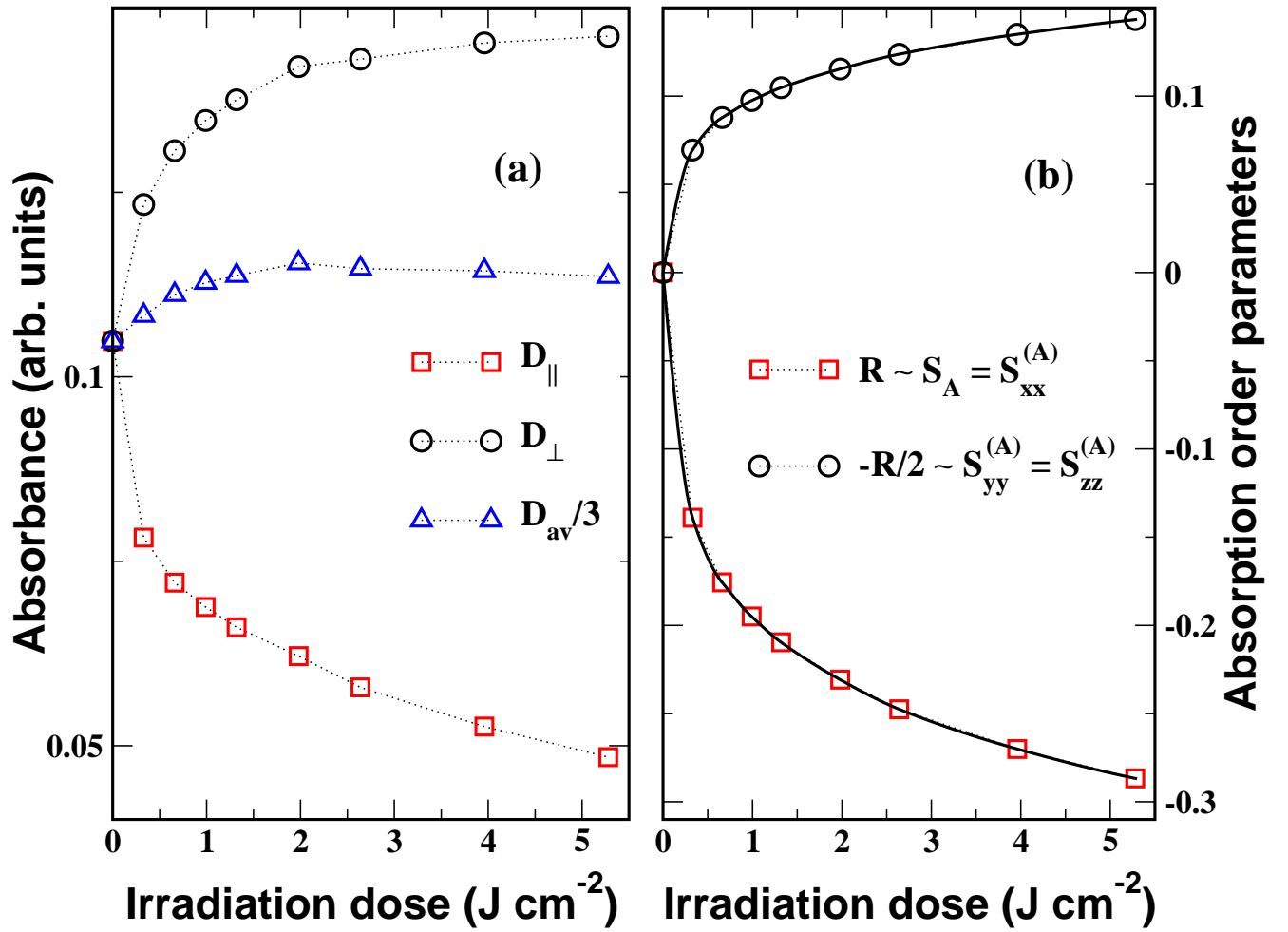


FIG. 5: Dependence of (a) absorption coefficients and (b) absorption order parameters on UV irradiation dose. Solid lines give interpolation of the experimental data calculated using Akima splines.

isotropic phase were injected into the cell by capillary action.

B. Absorption spectra

The UV-visible absorption spectra of the films were measured in the spectral range from 250 nm to 600 nm for the normally incident probing light which is linearly polarized parallel (along the x axis) and perpendicular (along the y axis) to the polarization vector of the activating light.

For nonirradiated films, the curve shown in Fig. 4 as a solid line demonstrates that the absorption coefficient does not depend on the polarization state of the testing beam. By contrast, as it is illustrated in Fig. 4, the absorption coefficients D_{\parallel} and D_{\perp} differ in the irradiated films, thus, revealing the light induced absorption dichroism. This dichroism is mainly caused by the photo-induced angular redistribution of the azo-dye molecules.

By varying the exposure time the films were prepared at different irradiation doses and the optical density components D_{\parallel} and D_{\perp} at the absorption maximum of azo-dyes ($\lambda_m \approx$

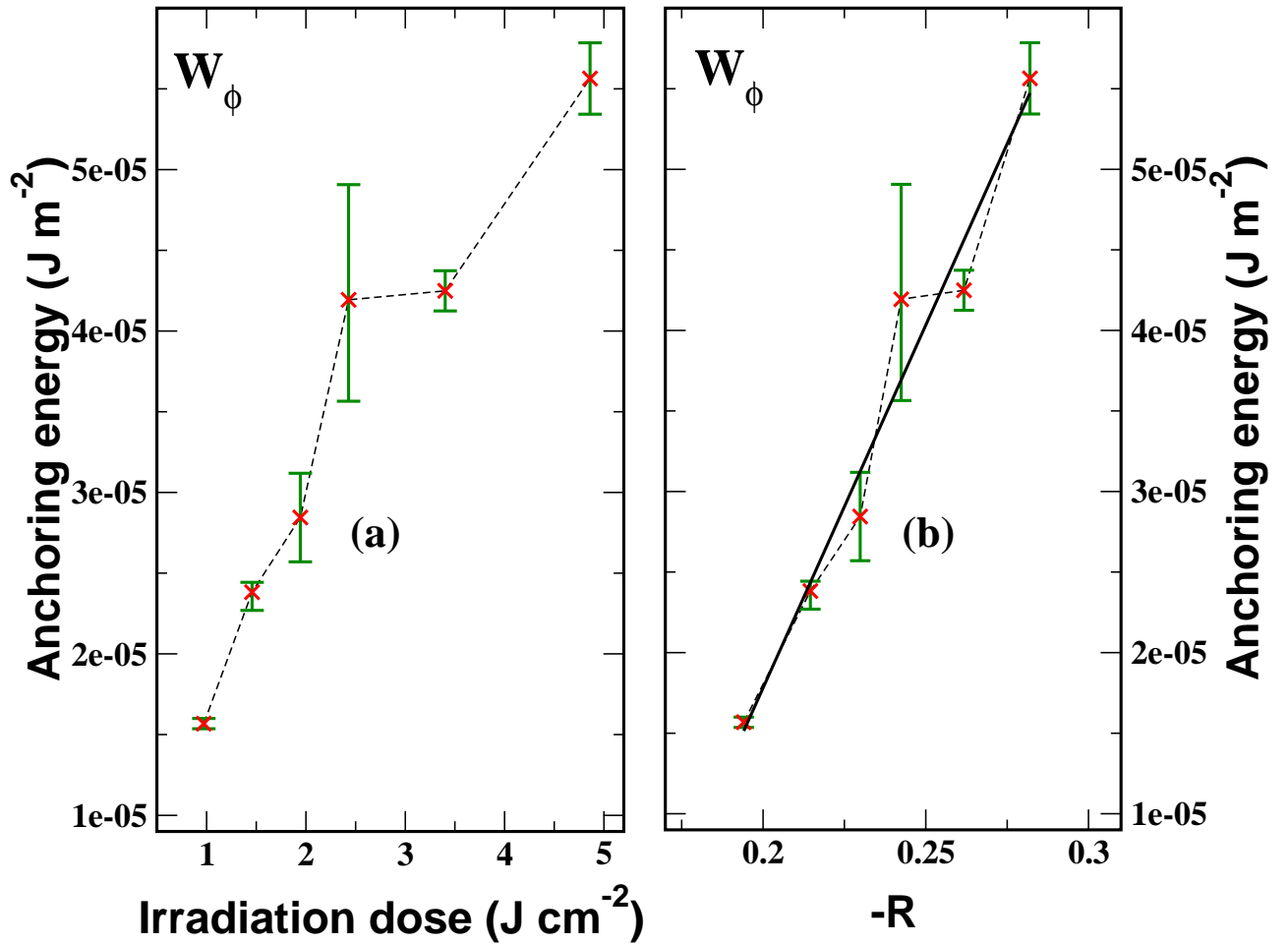


FIG. 6: Azimuthal anchoring energy as a function of (a) UV irradiation dose and (b) dichroic ratio (3) which is proportional to the order parameter of azo-dye molecules, S_A (see Eq. (9)). Solid line represents the result of linear fitting $W_\phi \approx -w_a^{(0)} - w_a^{(1)}R$ with $w_a^{(0)} = 0.07225$ mJ/m² and $w_a^{(1)} = 0.4503$ mJ/m².

350 nm) were estimated from the measured absorption spectra. The dichroic ratio then can be computed from the formula (3). The results for the absorption coefficients and the absorption order parameters, which are proportional to the dichroic ratio, are presented in Figs. 5(a) and 5(b), respectively.

C. Anchoring energy strengths

The azimuthal anchoring strength, W_ϕ , was measured in a twisted nematic cell using the torque balance method [42, 43]. The azo-dye aligning film and a rubbed polyimide layer were used as confining substrates. The twist angle was 90 degrees.

Measurements of the polar anchoring strength, W_θ , in anti-parallel aligned cells were carried out using the high-voltage technique [22, 44, 45, 46]. The experimental data for the azimuthal and polar anchoring strengths are plotted against the irradiation dose in Fig. 8(a) and Fig. 9(a), respectively. At low irradiation doses, when the exposure energy is below

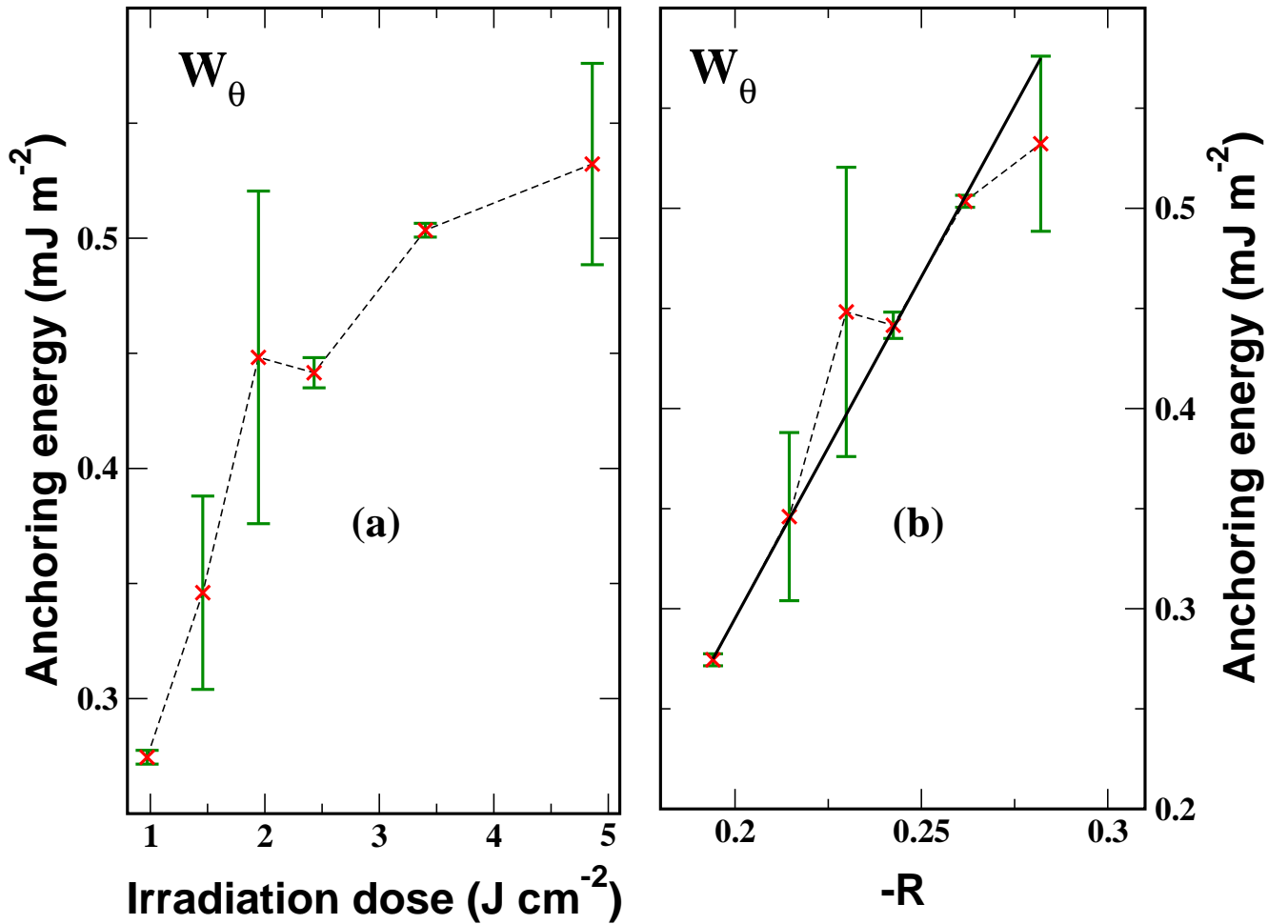


FIG. 7: Polar anchoring energy as a function of (a) UV irradiation dose and (b) dichroic ratio (3) which is proportional to the order parameter of azo-dye molecules, S_A (see Eq. (9)). Solid line represents the result of linear fitting $W_\theta \approx -w_p^{(0)} - w_p^{(1)} R$ with $w_p^{(0)} = 0.38714 \text{ mJ/m}^2$ and $w_p^{(1)} = 3.4116 \text{ mJ/m}^2$.

1 J/cm^2 , our experimental technique failed to provide accurate estimates for the anchoring strengths because of poor quality of NLC alignment in the cells.

The experimentally measured dependence of the dichroic ratio on the irradiation dose can now be combined with the results for W_ϕ and W_θ so as to recalculate the anchoring energy strengths as functions of the dichroic ratio, R . The resulting data are shown in Figs. 8(b) and 9(b).

IV. RESULTS

As is shown in Fig. 5(a) representing the absorption coefficients, D_\parallel and D_\perp , measured in the film irradiated at various irradiation doses, within the limits of experimental error, the average absorption coefficient, D_{av} , defined by the relation (8), remains unchanged at irradiation doses higher than 1 J/cm^2 . So, from the discussion given at the end of Sec. II A we conclude that the azo-dye order parameter in the bulk of the film is uniaxial and is of

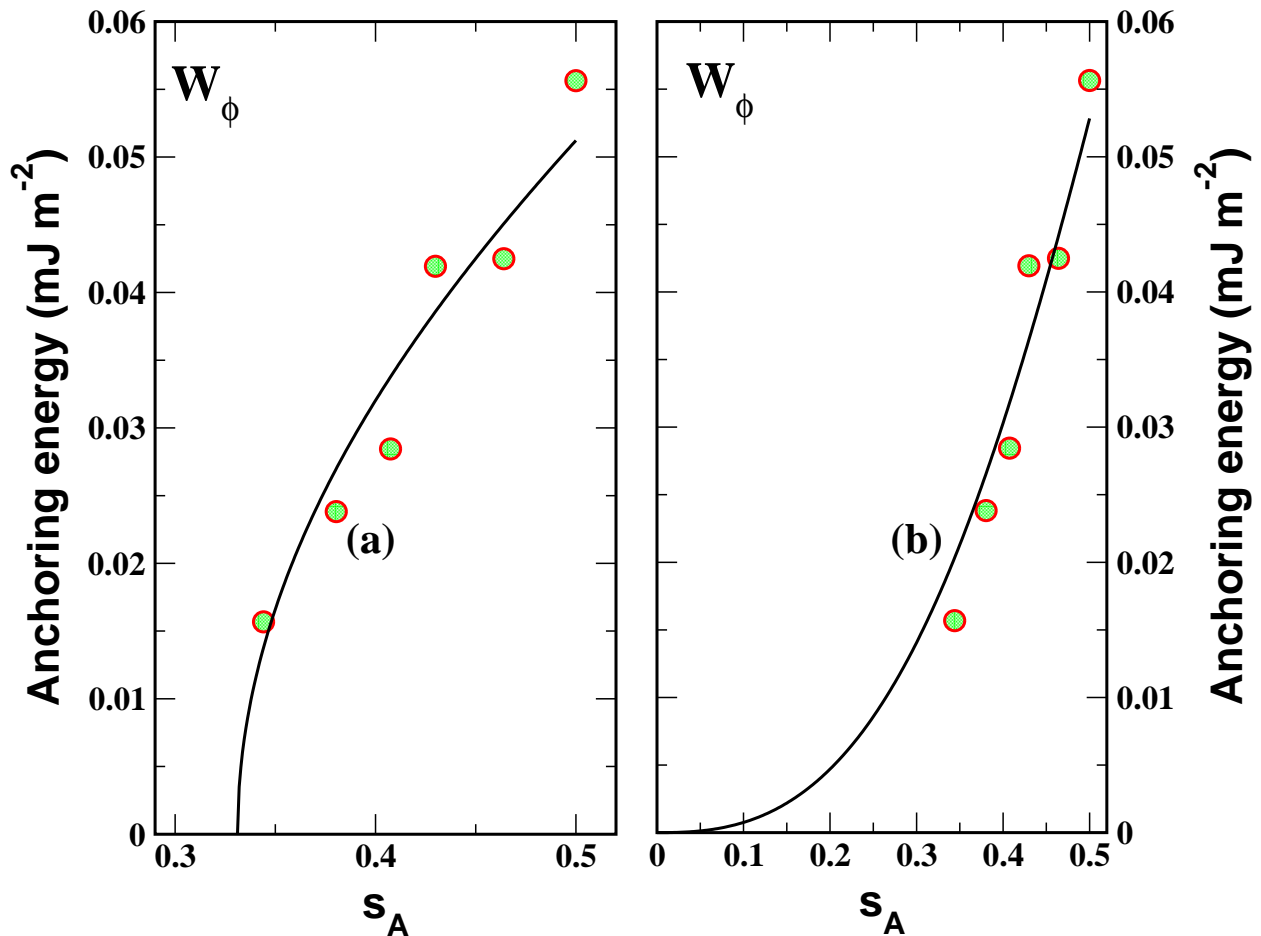


FIG. 8: Azimuthal anchoring energy versus azo-dye order parameter. Solid lines represent theoretical curves computed from the formula (30) by minimizing the energy (38) for two different sets of the parameters: (a) $g_1 = 0.47$, $g_2 = 0.4$, $w_\phi = 0.067 \text{ mJ/m}^2$; (b) $g_1 = -0.9$, $g_2 = 0.4$, $w_\phi = 0.157 \text{ mJ/m}^2$.

the form given by Eq. (9). In Fig. 5(b), it is indicated that the components of the order parameter tensor are proportional to the dichroic ratio (3). Clearly, for $D_\perp > D_\parallel$ and $\sigma_\parallel > \sigma_\perp$, the azo-dye order parameter S_A and R are both negative.

The experimental results for the azimuthal and polar anchoring strengths measured in NLC cells with photoaligned azo-dye films used as aligning substrates are presented in Figs. 6(a) and 7(a), respectively. The films differ in an amount of photoinduced anisotropy which is controlled by varying exposure time and the anchoring strengths are plotted in relation to the irradiation dose.

However, the fundamentally important characteristic describing degree of the photoinduced anisotropy is the azo-dye order parameter. So, in order to compare the experimental data and the theory, we need to relate the anchoring strengths and the dichroic ratio. Combining the anchoring energy data and the curve depicted in Fig. 5(b) gives the result shown in Figs. 6(b) and 7(b).

From the relations (30)-(33) the anchoring strengths depend linearly on the dichroic ratio provided the order parameters at the surface do not differ from their values in the bulk. The results of linear fitting of the experimental data are shown as solid straight lines in Figs. 6(b)

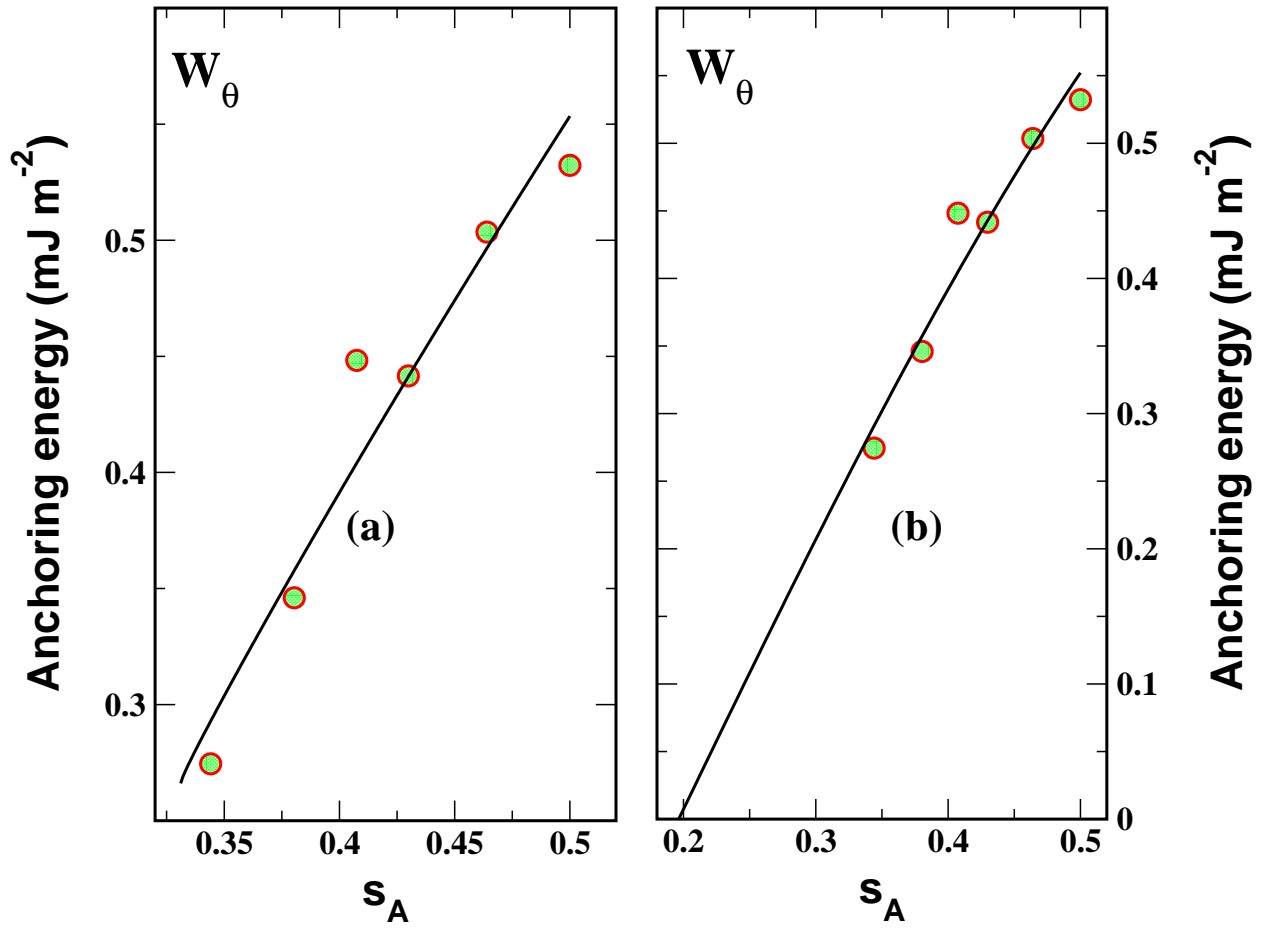


FIG. 9: Polar anchoring energy versus azo-dye order parameter. Solid lines represent theoretical curves computed from the formula (32) by minimizing the energy (38) for two different sets of the parameters: (a) $g_1 = 0.47$, $g_2 = 0.4$, $w_\theta^{(0)} = 1.113$ mJ/m², $w_\theta^{(1)} = 2.711$ mJ/m²; (b) $g_1 = -0.9$, $g_2 = 0.4$, $w_\theta^{(0)} = -0.382$ mJ/m², $w_\theta^{(1)} = 2.247$ mJ/m².

and 7(b).

Referring to Fig. 6(b), the linear approximation for W_ϕ predicts that the azimuthal anchoring strength vanish at certain non-zero value of the dichroic ratio, $R \approx -0.16$. By contrast, from the formulas (30) and (31) the anchoring strength W_ϕ is proportional to R and, thus, disappear only in the limit of weak photoinduced anisotropy where $R \rightarrow 0$. Assuming that this discrepancy can be attributed to the difference between the bulk and surface order parameters of azo-dye, we can apply the phenomenological model described in Sec. IID to interpret the experimental data.

In the angle-amplitude representation (35), the surface order parameters that enter the expression (30) are given by

$$S_{xx}^{(A)}|_{z=0} = -s_A \cos \psi_0, \quad S_{yy}^{(A)}|_{z=0} = s_A \cos(\psi_0 - \pi/3), \quad (45)$$

where $-s_A = S_A = (\Delta\sigma/\sigma_{av})R$ is the scalar order parameter in the bulk of the azo-dye film [see Eq. (9)]. According to our model, ψ_0 is the angle that minimizes the energy (38).

So, the computational procedure involves two steps: (a) minimization of the energy (38) to find the angle ψ_0 ; and (b) using the relations (45) to compute the azimuthal anchor-

ing energy (30). Following this procedure, we may calculate dependence of the anchoring strength W_ϕ on the photoinduced order parameter s_A .

As it is discussed in Sec. IID, the result crucially depend on the boundary conditions that are determined by two coupling constants, g_1 and g_2 . At $g_1 \geq 0$, the surface favors planar (random in-plane) alignment of the azo-dye molecules. In the opposite case of negative coupling constant g_1 , the alignment is homeotropic.

In figure 8, we show the theoretical curves calculated for both planar and homeotropic boundary conditions. The corresponding numerical results for the polar anchoring strength are presented in Fig. 9.

The curve plotted in Fig. 8(a) indicates that, for planar boundary conditions, the azimuthal anchoring strength W_ϕ takes non-zero values and starts growing only if the azo-dye order parameter s_A exceeds its critical value s_c . Such threshold behavior is a consequence of the second order transition discussed in Sec. IID. Contrastingly, as is shown in Fig. 8(b), W_ϕ is a smoothly increasing function of s_A when the boundary conditions favor the homeotropic alignment at the surface.

At first glance, the curves representing the polar anchoring strength W_θ plotted against s_A in Figs. 9(a)-(b) do not show any noticeable differences. It, however, should be stressed that the planar boundary conditions prevent the polar anchoring energy from decaying to zero as the order parameter s_A decreases. From Fig. 9(b) it can be seen that this is no longer the case when the coupling constant g_1 becomes negative.

These results show that interplay between photoinduced ordering in the bulk of the azo-dye films and the preferred alignment of the azo-dye molecules at the surface may have a profound effect on the order parameter dependence of the anchoring energies. For the planar alignment with $g_1 > 0$, our model predicts that the surface ordering may change through the second order transition as the photoinduced anisotropy increases. This transition bears close resemblance to the second order transitions in nematic liquid crystals previously studied in Refs. [47, 48].

Quantitatively, the polar anchoring energy W_θ appears to be an order of magnitude higher than the azimuthal energy W_ϕ . From our estimates, the ratio of the coefficients $w_\theta^{(1)}$ and w_ϕ , $w_\theta^{(1)}/w_\phi = -(c_A^{(2)} + c_A^{(3)})/c_A^{(1)}$, is likely to be well above 10.

The coefficient $c_A^{(1)}$ is negative and its sign is determined by the dominating contribution from the Maier-Saupe term v_{220} of the spherical harmonics expansion for the azo-dye – NLC intermolecular potential U_{A-N} . From Eq. (B10) the absolute value of $c_A^{(2)}$ can be significantly reduced when the quadrupole term v_{224} and the harmonics v_{222} are predominately positive, so that $\int_0^\infty z v_{224}(z) dz > 0$ and $\int_0^\infty z v_{222}(z) dz > 0$.

Under these circumstances, the condition (34), that requires the sum of $c_A^{(2)}$ and $c_A^{(3)}$ to be positive, can be satisfied only if the contribution of the quadrupole term to the sum $c_A^{(2)} + c_A^{(3)}$ is dominating. Thus, we may conclude that the quadrupole term is of vital importance for the understanding the reasons behind the significant difference in magnitude between the photoinduced parts of the polar and azimuthal anchoring strengths.

V. DISCUSSION AND CONCLUSIONS

In this paper we have studied both theoretically and experimentally effects of photoinduced ordering in the azo-dye aligning films on the anchoring energy strengths. These effects are governed by dependence of the strengths on the azo-dye order parameter.

Our theoretical approach relies on the mean field theory [28] and provides general expressions for the Landau-de Gennes surface free energy (13) and the anchoring energy (22). The theoretical results for the azimuthal and polar anchoring energy strengths are obtained under certain simplifying assumptions and used to interpret the experimental data relating the anchoring strengths and the dichroic ratio.

We found that linear fitting of the data for the azimuthal anchoring strength, though giving good results, predicts, in contradiction to the bare anchoring theory, the effect of vanishing anchoring which occurs at certain non-zero value of the dichroic ratio (and, thus, the irradiation dose). By using a simple phenomenological model we have shown that this effect can be attributed to an interplay between the light induced ordering in the bulk and the boundary conditions at the surface of the film which may counteract the action of light. Thus, the bulk and surface values of the azo-dye order parameter are generally different.

For planar boundary conditions that favor the random in-plane alignment of the azo-dye molecules, our model predicts threshold behavior of the azimuthal anchoring strength that starts growing provided the bulk order parameter, s_A , exceeds its critical value. When the boundary conditions are homeotropic, this is no longer the case and the azimuthal strength smoothly increases with the dichroic ratio.

The results presented in Figs. 8 and 9 demonstrate that the theoretical curves calculated for both types of the boundary conditions can fit the experimental data equally well. There are, however, differences concerning the polar anchoring strength. By contrast to the homeotropic boundary conditions, it never equals zero at the planar conditions. From the previously published results [22, 49] it can be concluded that the homeotropic boundary conditions is unlikely to occur in the azo-dye films under consideration.

Our final remark concerns some of the simplifying assumptions taken in our theoretical analysis. A more sophisticated theory that goes beyond the Fowler approximation (10) is required to take into account surface adsorption phenomena. A self-consistent treatment of two order parameter tensors in the interfacial layer also remains a challenge. We hope that our results will stimulate further progress in the field.

Acknowledgments

This research was partially supported by RGC grants HKUST6102/03E and HKUST6149/04E. A.D.K. is indebted to Professor T.J. Sluckin for numerous useful conversations and acknowledges partial support from INTAS under grant No. 03-51-5448. We are also grateful to Professor H.-S. Kwok for stimulating comments.

APPENDIX A: IRREDUCIBLE TENSORS, ORDER PARAMETER AND INVARIANTS

In this appendix we introduce notations and definitions used throughout the paper. In addition, we express the order parameter in terms of irreducible tensors and deduce a number of algebraic relations simplifying the derivation of the tensorial form of the intermolecular potential given in Appendix B.

The irreducible tensors, \mathbf{T}_m , with the azimuthal number m ranged from -2 to 2 can be

defined as linear combinations of the following form [50]:

$$\mathbf{T}_m = \sum_{\mu, \nu=-1}^1 C_{\mu\nu m}^{112} \mathbf{e}_\mu \otimes \mathbf{e}_\nu, \quad (\text{A1})$$

where $C_{m_1 m_2 m}^{j_1 j_2 j}$ is the Clebsch-Gordon (Wigner) coefficient and $\mathbf{e}_{\pm 1} = \mp(\hat{\mathbf{x}} \pm i\hat{\mathbf{z}})/\sqrt{2}$, $\mathbf{e}_0 = \hat{\mathbf{z}}$ are the vectors of spherical basis ($\hat{\mathbf{x}}$, $\hat{\mathbf{y}}$ and $\hat{\mathbf{z}}$ are the unit vectors directed along the corresponding coordinate axes). Substituting the values of the Wigner coefficient into Eq. (A1) gives the expressions for \mathbf{T}_m

$$\mathbf{T}_0 = (3\mathbf{e}_0 \otimes \mathbf{e}_0 - \mathbf{I})/\sqrt{6}, \quad (\text{A2})$$

$$\mathbf{T}_{\pm 1} = (\mathbf{e}_0 \otimes \mathbf{e}_{\pm 1} + \mathbf{e}_{\pm 1} \otimes \mathbf{e}_0)/\sqrt{2}, \quad (\text{A3})$$

$$\mathbf{T}_{\pm 2} = \mathbf{e}_{\pm 1} \otimes \mathbf{e}_{\pm 1}, \quad (\text{A4})$$

so that it is not difficult to verify the validity of the orthogonality relation

$$\text{Tr}[\mathbf{T}_m \mathbf{T}_{-n}] = (-1)^m \delta_{mn} \quad (\text{A5})$$

and the algebraic identities

$$\hat{\mathbf{z}} \cdot \mathbf{T}_m \cdot \hat{\mathbf{z}} = \sqrt{2/3} \delta_{m0}, \quad \hat{\mathbf{z}} \cdot \mathbf{T}_m \mathbf{T}_{-n} \cdot \hat{\mathbf{z}} = c_{|m|} \delta_{mn}, \quad (\text{A6})$$

where $c_0 = 2/3$, $c_1 = -1/2$ and $c_2 = 0$.

Under the action of rotation the vectors of spherical basis transform as follows

$$\mathbf{e}_\mu \rightarrow \mathbf{e}_\mu(\hat{\mathbf{u}}) = \sum_{\nu=-1}^1 D_{\nu\mu}^1(\hat{\mathbf{u}}) \mathbf{e}_\nu, \quad (\text{A7})$$

$$\mathbf{e}_0(\hat{\mathbf{u}}) = \hat{\mathbf{u}}, \quad (\text{A8})$$

$$\mathbf{e}_{\pm 1}(\hat{\mathbf{u}}) = \mp(\mathbf{e}_x(\hat{\mathbf{u}}) \pm i\mathbf{e}_y(\hat{\mathbf{u}}))/\sqrt{2}, \quad (\text{A9})$$

where $D_{nm}^j(\hat{\mathbf{u}}) \equiv D_{nm}^j(\theta, \phi)$ is the Wigner D function [50, 51]; θ and ϕ are Euler angles of the unit vector $\hat{\mathbf{u}}$; $\mathbf{e}_x(\hat{\mathbf{u}}) = (\cos \theta \cos \phi, \cos \theta \sin \phi, -\sin \theta)$, $\mathbf{e}_y(\hat{\mathbf{u}}) = (-\sin \phi, \cos \phi, 0)$.

The definition (A1) implies that transformation properties of the tensors \mathbf{T}_m under rotations are determined by the irreducible representation of the rotation group with $j = 2$, where j is the angular momentum number. So, we have

$$\mathbf{T}_m \rightarrow \mathbf{T}_m(\hat{\mathbf{u}}) = \sum_{\mu, \nu=-1}^1 C_{\mu\nu m}^{112} \mathbf{e}_\mu(\hat{\mathbf{u}}) \otimes \mathbf{e}_\nu(\hat{\mathbf{u}}) = \sum_{k=-2}^2 D_{km}^2(\hat{\mathbf{u}}) \mathbf{T}_k. \quad (\text{A10})$$

Eq. (A10) can now be combined with the relations (A8) and (A2) to yield the expression for the order parameter tensor $\mathbf{Q}(\hat{\mathbf{u}})$:

$$\mathbf{Q}(\hat{\mathbf{u}}) = \sqrt{3/2} \mathbf{T}_0(\hat{\mathbf{u}}) = (3\hat{\mathbf{u}} \otimes \hat{\mathbf{u}} - \mathbf{I})/2, \quad (\text{A11})$$

where the unit vector $\hat{\mathbf{u}}$ is directed along the long molecular axis.

The director $\hat{\mathbf{n}}$ is defined as an eigenvector of the orientationally averaged order parameter tensor

$$\langle \mathbf{Q}(\hat{\mathbf{u}}) \rangle_{\hat{\mathbf{u}}} = \sqrt{3/2} \sum_{k=-2}^2 \langle D_{k0}^2(\phi', \theta') \rangle \mathbf{T}_k(\hat{\mathbf{n}}), \quad (\text{A12})$$

where θ' and ϕ' are Euler angles of the vector $\hat{\mathbf{u}}$ related to the basis vectors $\mathbf{e}_i(\hat{\mathbf{n}})$.

Since $\hat{\mathbf{n}}$ is the director, the averages $\langle D_{\pm 10}^2(\phi', \theta') \rangle_{\phi', \theta'}$ vanish. Other averages

$$\langle D_{00}^2(\phi', \theta') \rangle = \sqrt{2/3} S, \quad (\text{A13})$$

$$\langle D_{\pm 20}^2(\phi', \theta') \rangle = P \exp(\pm 2i\gamma) / \sqrt{6} \quad (\text{A14})$$

are proportional to the scalar order parameter S and the biaxiality parameter P .

By using the orthogonality conditions (A5) and Eqs. (A12)-(A14) we recover the relations in the traditional form [30]:

$$\langle \mathbf{Q}(\hat{\mathbf{u}}) \rangle_{\hat{\mathbf{u}}} \equiv \mathbf{S}(\hat{\mathbf{n}}) = S \mathbf{Q}(\hat{\mathbf{n}}) + P(\hat{\mathbf{m}} \otimes \hat{\mathbf{m}} - \hat{\mathbf{l}} \otimes \hat{\mathbf{l}}) / 2, \quad (\text{A15})$$

$$S = \left\langle 3 (\hat{\mathbf{u}} \cdot \hat{\mathbf{n}})^2 - 1 \right\rangle / 2, \quad (\text{A16})$$

$$P = 3 \left\langle (\hat{\mathbf{u}} \cdot \hat{\mathbf{m}})^2 - (\hat{\mathbf{u}} \cdot \hat{\mathbf{l}})^2 \right\rangle / 2, \quad (\text{A17})$$

where $\hat{\mathbf{m}} = \cos \gamma \mathbf{e}_x(\hat{\mathbf{n}}) - \sin \gamma \mathbf{e}_y(\hat{\mathbf{n}})$ and $\hat{\mathbf{l}} = \sin \gamma \mathbf{e}_x(\hat{\mathbf{n}}) + \cos \gamma \mathbf{e}_y(\hat{\mathbf{n}})$.

The order parameter (A15) is a traceless symmetric tensor. Therefore, there are two non-vanishing independent invariants

$$I_2 = \text{Tr}[\mathbf{S}^2(\hat{\mathbf{n}})] = (3S^2 + P^2) / 2, \quad (\text{A18})$$

$$I_3 = \text{Tr}[\mathbf{S}^3(\hat{\mathbf{n}})] = 3S(S^2 - P^2) / 4, \quad (\text{A19})$$

which enter the non-elastic part of the well known phenomenological expression for the Landau-de Gennes free energy density

$$f_{\text{LG}} = \frac{2a}{3} (T - T^*) I_2 - \frac{4B}{3} I_3 + \frac{4C}{9} I_2^2, \quad (\text{A20})$$

where T is the temperature and T^* is the supercooling temperature.

For the scalar order parameters (A16) and (A17) combined into a pair (S, P) , it is convenient to introduce what might be called the ‘‘polar’’ (or amplitude-angle) representation

$$S = s \cos \psi, \quad P = \sqrt{3} s \sin \psi, \quad (\text{A21})$$

where $s^2 = 2I_2/3$. Using the representation (A21) the free energy density (A20) can be recast into the form

$$f_{\text{LG}}(s, \psi) = a(T - T^*)s^2 - Bs^3 \cos(3\psi) + Cs^4 \equiv B^2 C^{-1} U_{\text{LG}}, \quad (\text{A22})$$

$$U_{\text{LG}}(\eta, \psi) = \frac{8+t}{32} \eta^2 - \eta^3 \cos(3\psi) + \eta^4, \quad \eta \equiv \frac{C}{B} s, \quad (\text{A23})$$

where $t = 32aCB^{-2}(T - T_c)$ is the dimensionless temperature parameter and $T_c = T^* + B^2/(4aC)$ is the temperature of the bulk nematic-isotropic transition. The rescaled

density (A23) is a generalized version of the dimensionless free energy density previously used in Refs. [47, 48].

Finally, we write down the components of the order parameter tensor (A16) in the polar representation

$$S_{ij} = s [n_i n_j \cos \psi + m_i m_j \cos(\psi - 2\pi/3) + l_i l_j \cos(\psi + 2\pi/3)] \quad (\text{A24})$$

and notice that the stationary points of the free energy density (A22) where the angle ψ is a multiple of $\pi/3$ represent uniaxially anisotropic states. The latter immediately recovers the well known result about uniaxial anisotropy of NLC equilibrium states [52].

APPENDIX B: TENSORIAL FORM OF INTERMOLECULAR POTENTIAL

We begin with the intermolecular potential between two rigid, axially symmetric molecules expanded in a series of spherical harmonics as follows [53]

$$U(\mathbf{r}, \hat{\mathbf{u}}_1, \hat{\mathbf{u}}_2) = \sum_{j_1, j_2, j} u_{j_1 j_2 j}(r) \sum_{m_1, m_2, m} C_{m_1 m_2 m}^{j_1 j_2 j} \times Y_{j_1 m_1}(\hat{\mathbf{u}}_1) Y_{j_2 m_2}(\hat{\mathbf{u}}_2) Y_{j m}^*(\hat{\mathbf{r}}) \quad (\text{B1})$$

where $\mathbf{r} \equiv \mathbf{r}_{12} = \mathbf{r}_1 - \mathbf{r}_2$, \mathbf{r}_i and $\hat{\mathbf{u}}_i$ are the position and orientation (equivalently, Euler angles of the long molecular axis) coordinates of the interacting molecules, respectively; $Y_{jm}(\hat{\mathbf{u}}) = \sqrt{(2j+1)/(4\pi)} D_{m0}^{j*}(\hat{\mathbf{u}})$ is the spherical function [50, 54]. The form of the expansion (B1) implies that the potential is invariant under translations, $\mathbf{r}_i \rightarrow \mathbf{r}_i + \Delta\mathbf{r}$, and rotations, $\{\mathbf{r}_i, \hat{\mathbf{u}}_i\} \rightarrow \{R\mathbf{r}_i, R\hat{\mathbf{u}}_i\}$. In addition, we shall assume the head-tail symmetry

$$U(\mathbf{r}, \hat{\mathbf{u}}_1, \hat{\mathbf{u}}_2) = U(\mathbf{r}, -\hat{\mathbf{u}}_1, \hat{\mathbf{u}}_2) = U(\mathbf{r}, \hat{\mathbf{u}}_1, -\hat{\mathbf{u}}_2), \quad (\text{B2})$$

so that the outer sum in Eq. (B1) is restricted to run over even values of j_1 and j_2 .

It is now our task to link the pairwise potential integrated over in-plane coordinates

$$\begin{aligned} V(z, \hat{\mathbf{u}}_1, \hat{\mathbf{u}}_2) &= \int_S U(\mathbf{r}, \hat{\mathbf{u}}_1, \hat{\mathbf{u}}_2) dx dy \\ &= \sum_{j_1, j_2, j} [(2j_1 + 1)(2j_2 + 1)(2j + 1)/(4\pi)^3]^{1/2} \\ &\times v_{j_1 j_2 j}(z) \sum_m C_{m - m 0}^{j_1 j_2 j} D_{m0}^{j_1}(\hat{\mathbf{u}}_1) D_{-m0}^{j_2}(\hat{\mathbf{u}}_2) D_{00}^j(\hat{\mathbf{z}}) \end{aligned} \quad (\text{B3})$$

and the tensorial representation that was originally suggested by Ronis and Rosenblatt in Ref. [34]

$$\begin{aligned} V(z, \hat{\mathbf{u}}_1, \hat{\mathbf{u}}_2) &\equiv V(z, \mathbf{Q}_1, \mathbf{Q}_2) = V_{\text{iso}}(z) + \beta^{(0)}(z) \hat{\mathbf{z}} \cdot (\mathbf{Q}_1 + \mathbf{Q}_2) \cdot \hat{\mathbf{z}} \\ &+ \beta^{(1)}(z) \text{Tr}(\mathbf{Q}_1 \mathbf{Q}_2) + \beta^{(2)}(z) \hat{\mathbf{z}} \cdot \mathbf{Q}_1 \mathbf{Q}_2 \cdot \hat{\mathbf{z}} \\ &+ \beta^{(3)}(z) [\hat{\mathbf{z}} \cdot \mathbf{Q}_1 \cdot \hat{\mathbf{z}}][\hat{\mathbf{z}} \cdot \mathbf{Q}_2 \cdot \hat{\mathbf{z}}], \end{aligned} \quad (\text{B4})$$

where $\mathbf{Q}_i \equiv \mathbf{Q}(\hat{\mathbf{u}}_i)$ is defined by Eq. (A11). In other words, the problem is to express the coefficients $\beta^{(i)}(z)$ in terms of the harmonics $v_{j_1 j_2 j}(z)$. To this end we restrict ourselves to

the lowest order harmonics of the expansion (B3) with $j_i < 4$ and consider the equation

$$x_1 [\hat{\mathbf{z}} \cdot \mathbf{T}_0(\hat{\mathbf{u}}_1) \cdot \hat{\mathbf{z}}][\hat{\mathbf{z}} \cdot \mathbf{T}_0(\hat{\mathbf{u}}_2) \cdot \hat{\mathbf{z}}] + x_2 \text{Tr}(\mathbf{T}_0(\hat{\mathbf{u}}_1)\mathbf{T}_0(\hat{\mathbf{u}}_2)) \\ + x_3 \hat{\mathbf{z}} \cdot \mathbf{T}_0(\hat{\mathbf{u}}_1)\mathbf{T}_0(\hat{\mathbf{u}}_2) \cdot \hat{\mathbf{z}} = \sum_{m=0}^2 \alpha_m D_{m0}^2(\hat{\mathbf{u}}_1) D_{-m0}^2(\hat{\mathbf{u}}_2), \quad (\text{B5})$$

that need to be solved for x_1 , x_2 and x_3 . The sum on the right hand side of Eq. (B5) represents sum of the harmonics with $j_1 = j_2 = 2$. The case of the harmonics with $j_1 j_2 = 0$ is much easier to treat as we only have to use the relation

$$\hat{\mathbf{z}} \cdot \mathbf{T}_0(\hat{\mathbf{u}}) \cdot \hat{\mathbf{z}} = D_{00}^2(\hat{\mathbf{u}}). \quad (\text{B6})$$

By using Eq. (A10) combined with the relations (A5) and (A6) it is straightforward to transform Eq. (B5) into a system of linear equations. The solution of the system is given by

$$x_1 = (3\alpha_0 + 4\alpha_1 + \alpha_2)/2, \\ x_2 = -2(\alpha_1 + \alpha_2), \\ x_3 = \alpha_2. \quad (\text{B7})$$

Given the values of the Wigner coefficients, we can now use the relations (B6) and (B7) to derive the final result in the following form:

$$V_{\text{iso}}(z) = v_{000}(z)/(4\pi)^{3/2}, \quad (\text{B8})$$

$$[(4\pi)^{3/2}/5] \beta^{(0)}(z) = v_{202}(z) = v_{022}(z), \quad (\text{B9})$$

$$[(4\pi)^{3/2}/5] \beta^{(1)}(z) = 2/(3\sqrt{5})\{v_{220}(z) \\ + 10/\sqrt{14} v_{222}(z) + 3/\sqrt{14} v_{224}(z)\}, \quad (\text{B10})$$

$$[(4\pi)^{3/2}/5] \beta^{(2)}(z) = -20/\sqrt{70}\{v_{222}(z) + v_{224}(z)\}, \quad (\text{B11})$$

$$[(4\pi)^{3/2}/5] \beta^{(3)}(z) = 35/\sqrt{70} v_{224}(z). \quad (\text{B12})$$

The formulas (B8)–(B12) relate the parameters of the representation (B4) to the coefficient functions in the spherical harmonics expansion (B3). The terms v_{202} and v_{022} describe the coupling between orientation of the molecules and the intermolecular vector, whereas v_{220} and v_{224} are known as the Maier-Saupe and the quadrupole terms, respectively. For the interaction between NLC molecules, the functions $\beta^{(1)}(z)$ and $\beta^{(2)}(z)$ define the elastic coefficients of NLC that must be positive. This stability condition implies that $\beta^{(1)}$ and $\beta^{(2)}$ are both predominately non-positive [27, 28, 31, 55].

[1] T. J. Sluckin and A. Poniewierski, in *Fluid Interfacial Phenomena*, edited by C. A. Croxton (Wiley, Chichester, 1986), chap. 5, pp. 215–253.

- [2] B. Jérôme, Rep. Prog. Phys. **54**, 391 (1991).
- [3] G. Barbero and G. Durand, in *Liquid Crystals in Complex Geometries*, edited by G. P. Crawford and S. Žumer (Taylor & Francis, London, 1996), chap. 2, pp. 21–52.
- [4] V. G. Chigrinov, *Liquid crystal devices: Physics and Applications* (Artech House, Boston, 1999).
- [5] W. M. Gibbons, P. J. Shannon, S.-T. Sum, and B. J. Swetlin, Nature **351**, 49 (1991).
- [6] M. Schadt, K. Schmitt, V. Kozinkov, and V. Chigrinov, Jpn. J. Appl. Phys. **31**, 2155 (1992).
- [7] A. Dyadyusha, T. Marusii, Y. Reznikov, V. Reshetnyak, and A. Khizhnyak, JETP Lett. **56**, 17 (1992).
- [8] M. O’Neill and S. M. Kelly, J. Phys. D: Appl. Phys. **33**, R67 (2000).
- [9] S. Furumi, M. Nakagawa, S. Morino, and K. Ichimura, Appl. Phys. Lett. **74**, 2438 (1999).
- [10] H. G. Galabova, D. W. Allender, and J. Chen, Phys. Rev. E **55**, 1627 (1996).
- [11] S. Perny, P. L. Barny, J. Delaire, T. Buffeteau, C. Sourisseau, I. Dozov, S. Forget, and P. Martinot-Lagarde, Liq. Cryst. **27**, 329 (2000).
- [12] O. Yaroshchuk, T. Sergan, J. Kelly, and I. Gerus, Jpn. J. Appl. Phys. **41**, 275 (2002).
- [13] A. Petry, S. Kummer, H. Anneser, F. Feiner, and C. Bräuchle, Ber. Bunsenges. Phys. Chem. **97**, 1281 (1993).
- [14] N. C. R. Holme, P. S. Ramanujam, and S. Hvilsted, Applied Optics **35**, 4622 (1996).
- [15] L. Blinov, M. Kozlovsky, M. Ozaki, K. Sarp, and K. Yoshino, J. Appl. Phys. **84**, 3860 (1998).
- [16] Y. Wu, J.-I. Mamiya, O. Tsutsumi, A. Kanazawa, T. Shiono, and T. Ikeda, Liq. Cryst. **27**, 749 (2000).
- [17] O. Yaroshchuk, A. D. Kiselev, Y. Zakrevskyy, J. Stumpe, and J. Lindau, Eur. Phys. J. E **6**, 57 (2001).
- [18] O. Yaroshchuk, T. Sergan, J. Lindau, S. N. Lee, J. Kelly, and L.-C. Chien, J. Chem. Phys. **114**, 5330 (2001).
- [19] O. V. Yaroshchuk, A. D. Kiselev, Y. Zakrevskyy, T. Bidna, J. Kelly, L.-C. Chien, and J. Lindau, Phys. Rev. E **68**, 011803 (2003).
- [20] V. G. Chigrinov, V. M. Kozenkov, and H. S. Kwok, in *Optical applications in photoaligning*, edited by L. Vicari (Inst. of Physics, Bristol, UK, 2003), pp. 201–244.
- [21] V. Chigrinov, E. Prudnikova, V. Kozenkov, H. Kwok, H. Akiyama, T. Kawara, H. Takada, and H. Takatsu, Liq. Cryst. **29**, 1321 (2002).
- [22] V. Chigrinov, A. Muravskii, and H. S. Kwok, Phys. Rev. E **68**, 061702 (2003).
- [23] L. T. Thieghi, R. Barberi, J. J. Bonvent, E. A. Oliveira, J. A. Giacometti, and D. T. Balogh, Phys. Rev. E **67**, 041701 (2003).
- [24] S. Oka, T. Mitsumoto, M. Kimura, and T. Akahane, Phys. Rev. E **69**, 061711 (2004).
- [25] O. V. Yaroshchuk, A. D. Kiselev, J. Lindau, V. Y. Reshetnyak, A. G. Tereshchenko, and Y. A. Zakrevskyy, Ukr. Fiz. Zhurnal **46**, 449 (2001).
- [26] A. L. Alexe-Ionescu, R. Barberi, M. Iovane, and A. T. Ionescu, Phys. Rev. E **65**, 011703 (2001).
- [27] A. K. Sen and D. E. Sullivan, Phys. Rev. A **35**, 1391 (1987).
- [28] P. I. C. Teixeira and T. J. Sluckin, J. Chem. Phys. **97**, 1490 (1992).
- [29] P. I. C. Teixeira and T. J. Sluckin, J. Chem. Phys. **97**, 1510 (1992).
- [30] P. G. de Gennes and J. Prost, *The Physics of Liquid Crystals* (Clarendon Press, Oxford, 1993).
- [31] M. A. Osipov and S. Hess, J. Chem. Phys. **99**, 4181 (1993).
- [32] M. A. Osipov and T. J. Sluckin, J. Phys. II France **3**, 793 (1993).

- [33] M. A. Osipov, T. J. Sluckin, and S. J. Cox, Phys. Rev. E **55**, 464 (1997).
- [34] D. Ronis and C. Rosenblatt, Phys. Rev. A **21**, 1687 (1980).
- [35] W. Zao, C.-X. Wu, and M. Iwamoto, Phys. Rev. E **62**, R1481 (2000).
- [36] W. Zhao, C.-X. Wu, and M. Iwamoto, Phys. Rev. E **65**, 031709 (2002).
- [37] Y. Guo-Chen, Z. Shu-Jing, H. Li-Jun, and G. Rong-Hua, Liq. Cryst. **31**, 1093 (2004).
- [38] I. F. Lyuksyutov, Sov. Phys.-JETP **48**, 178 (1978).
- [39] E. Penzenstadler and H.-R. Trebin, J. Phys. (France) **50**, 1027 (1989).
- [40] R. Rosso and E. Virga, J. Phys. A: Math. Gen. **29**, 4247 (1996).
- [41] S. Kralj and E. Virga, J. Phys. A: Math. Gen. **34**, 829 (2001).
- [42] Y. Iimura, N. Kobayashi, and S. Kobayashi, Jpn. J. Appl. Phys. **34**, 1935 (1995).
- [43] V. P. Vorflusev, H.-S. Kitzerow, and V. Chigrinov, Jpn. J. Appl. Phys. **34**, L1137 (1995).
- [44] H. Yokoyama and H. A. van Sprang, J. Appl. Phys. **57**, 4520 (1985).
- [45] Y. A. Nastishin, R. D. Polak, S. V. Shiyankovskii, V. H. Bodnar, and O. D. Lavrentovich, J. Appl. Phys. **86**, 4199 (1999).
- [46] H. Yokoyama and R. Sun, Jpn. J. Appl. Phys. **39**, L45 (2000).
- [47] P. Sheng, B.-Z. Li, M. Zhou, T. Mose, and Y. R. Shen, Phys. Rev. A **46**, 946 (1992).
- [48] T. Z. Qian and P. Sheng, Phys. Rev. E **55**, 7111 (1997).
- [49] A. Murauski, V. Chigrinov, A. Muravsky, F. S.-Y. Yeung, J. Ho, and H.-S. Kwok, Phys. Rev. E **71**, 061707 (2005).
- [50] L. C. Biedenharn and J. D. Louck, *Angular Momentum in Quantum Physics* (Addison–Wesley, Reading, Massachusetts, 1981).
- [51] I. M. Gelfand, R. A. Minlos, and Z. Y. Shapiro, *Representations of Rotation and Lorentz Groups and Their Applications* (Pergamon Press, Oxford, 1963).
- [52] A. Z. Patashinskii and V. L. Pokrovskii, *Fluctuational Theory of Phase Transitions* (Nauka, Moscow, 1982), 2nd ed., (in Russian).
- [53] J. A. Pople, Proc. R. Soc. Lond. A **221**, 498 (1954).
- [54] M. Abramowitz and I. A. Stegun, eds., *Handbook of Mathematical Functions* (Dover, New York, 1972).
- [55] B. Tjijto-Margo and D. E. Sullivan, J. Chem. Phys. **88**, 6620 (1988).